## ABSTRACT

McCORMICK, CAROLYN MARIE. Altered Trabecular Microarchitecture near the Glenohumeral Joint in a Rat Model of Neonatal Brachial Plexus Injury. (Under the direction of Jacqueline Cole and Katherine Saul).

Neonatal brachial plexus injury (NBPI) occurs in nearly 1.5 of every 1000 infants during childbirth (Foad, Mehlman, & Ying, 2008), and 30-40% of these neonates sustain impaired function in the affected arm throughout their lifespan (Abzug, Kozin, & Zlotolow, 2015). Severity of upper limb paresis following NBPI may lead to reduced passive and active range of motion, including internal rotation contracture at the shoulder or flexion contracture at the elbow (Reading, Laor, Salisbury, Lippert, & Cornwall, 2012). Despite full neurologic recovery in 80-90% of affected children (Pearl, 2009), secondary glenohumeral deformities may still limit arm movement and hinder critical activities of daily living, such as eating and bathing. Abnormal development of muscle and bone at the shoulder is the most common reason for surgical intervention post-injury to improve functional outcomes (Abzug *et al*., 2015). However, very little is understood about parallel postnatal development of muscle and bone after peripheral nerve injury despite evidence that musculoskeletal deformities constrain movement, even after restored neurological function. Consequently, clinical management of secondary musculoskeletal deformity in the injured extremity has variable functional outcomes (Kozin, 2010). Regions in the glenohumeral joint experiencing abnormal growth and morphological deformities are comprised primarily of cancellous bone, which is integral to transfer of joint loading along the bone and is known to adapt to altered loads (Wolff, 1892/1986; Frost, 1994). This thesis examines underlying changes in cancellous bone in the glenohumeral joint using a rat model of NBPI.

Sixteen Sprague-Dawley rat pups (Harlan Laboratories, Indianapolis, Indiana) received either neurectomy or sham surgery (*n*=8 each) five days postnatal in a prior study (Crouch *et al*., 2015). We assessed trabecular bone metrics, specifically bone mineral density (BMD), tissue mineral density (TMD), bone volume fraction (BV/TV), trabecular number (Tb.N), trabecular thickness and separation (Tb.Th, and Tb.Sp) and their standard deviations (Tb.Th.SD, Tb.Sp.SD) using direct 3D methods (Bouxsein *et al.*, 2010). Differences between neurectomy and sham groups were analyzed using two-tailed, unpaired t-tests. Differences between affected and contralateral limbs were analyzed using two-tailed, paired t-tests. Correlations between gross morphological bone measurements (humeral head superoinferior and anteroposterior translation and glenoid version and inclination) and trabecular bone metrics in the neurectomy scapulae and humeri were assessed using Pearson correlation tests.

Changes in trabecular bone density and microarchitecture were similar in the humeral epiphysis and metaphysis. Trabecular TMD tended to be 4.5% lower in the neurectomy group than in the sham group (p=0.072 epiphysis, p=0.12 metaphysis). Trabecular thickness tended to be 12.5% lower in neurectomy relative to sham (p=0.076 epiphysis, p=0.057 metaphysis). BV/TV was not significantly different between groups (p=0.27 epiphysis, p=0.27 metaphysis), despite observing 14.4% reduction for neurectomy.

Cancellous bone deterioration following neurectomy was also observed in the scapular glenoid. Relative to sham, the neurectomy group had significantly lower BV/TV (-18.6% in zone 2 in inferior glenoid underlying the fossa, p=0.0027) and Tb.N (-17.5 % in zone 3 in inferior glenoid near glenoid rim, p=0.011) and greater Tb.Sp (28.8% in zone 1 in subcoracoid region forming the superior glenoid, p=0.029 and 31.6% in zone 3, p=0.020). A trend for reduced BV/TV was observed in zone 3 (-4.95%) in neurectomy relative to sham (p=0.062).

This thesis demonstrated that NBPI affects trabecular microarchitecture in addition to overall bone morphology. Our findings align with other reports of compromised trabecular bone following NBPI (Kim, Galatz, Das, Patel, & Thomopoulos, 2010). Further investigation is needed to understand whether NBPI causes overall weaker bone strength in the shoulder. A more in-depth understanding about postnatal glenohumeral development may inform therapies and treatments that maximize shoulder movement and minimize bone damage.

# Altered Trabecular Microarchitecture near the Glenohumeral Joint of a Rat Model with Neonatal Brachial Plexus Injury

by
Carolyn Marie McCormick

A thesis submitted to the Graduate Faculty of
North Carolina State University
in partial fulfillment of the
requirements for the degree of
Master of Science

Biomedical Engineering

Raleigh, North Carolina

2017

APPROVED BY:

| | |
|---|---|
| _____ | _____ |
| Dr. Jacqueline Cole | Dr. Katherine Saul |
| Co-Chair of Advisory Committee | Co-Chair of Advisory Committee |

_____
Dr. Gregory Sawicki

## DEDICATION

I would like to dedicate my thesis to those who have inspired me along this journey:

To those who have endured brachial plexus injury at birth – May you and your loved ones know that the study described herein is part of a larger goal to minimize and one day, eradicate the suffering from your injury. I am inspired to work hard as you persevere through good and bad days.

To my mom and dad – Thank you for showing me your unconditional love and teaching me to love as Christ Jesus has taught us. From you, Dad, I owe my curiosity for all things technical and scientific as well as the insatiable desire to give others my very best work. From you, Mom, I admire your compassion for your young students, your friends, and our family. I have learned to approach biomedical research with a tender heart because of yours.

To my grandma (with the bun!) – I love our weekly phone calls and the beautiful cards you send me. Your long tenure as a nurse for patients with paraplegia and quadriplegia has inspired me to pursue a career that is committed to improving the well-being of others through biomedical innovations.

To my family and friends – Thank you for keeping me grounded and reminding me to celebrate the little victories in my work and life. You bring me joy and encouragement.

To Matt – I am so blessed that you are my husband. I love you for your faith in God, your kindness to others, your strong work ethic in all things, and your unwavering commitment to open-source, reproducible research. I am glad to have you by my side as I strive to become my best self.

"We are each called to reach out to others. On rare occasions that can happen on a grand scale. But most of the time it happens in simple acts of kindness of one person to another. Those are the events that really matter." – Francis S. Collins, *The Language of God: A Scientist Presents Evidence for Belief*, p. 286.

"[T]he simple act of trying to help just one person, in a desperate situation where my skills were poorly matched to the challenge, turned out to represent the most meaningful of all human experiences. A burden lifted. This was true north. And the compass was not pointed at self-glorification, or at materialism, or even at medical science – instead, it pointed at the goodness that we all hope desperately to find within ourselves and others. I also saw more clearly than ever before the author of that goodness and truth, the real True North, God himself, revealing His holy nature by the way in which He has written this desire to seek goodness in all of our hearts." – Francis S. Collins, *The Language of God: A Scientist Presents Evidence for Belief*, pp. 287-288.

## BIOGRAPHY

Carolyn Marie McCormick (née Stolfi) was born in Queens, New York, and raised in Chatham, New Jersey. From a young age, she delighted in scientific endeavors. In a 1st grade Halloween parade, little Carolyn proudly marched as a self-proclaimed 'serious scientist' in her father's white collar shirt that had been repurposed as an oversized lab coat and a pair of her grandfather's old specs with missing lenses.

In 2009, Carolyn completed a Bachelor of Science degree in mechanical engineering at Lafayette College in Easton, PA. There, she learned that technology development and biomedical research could help people in ways she never imagined. Her academic journey continued at Purdue University in West Lafayette, IN, where she studied haptics, or the science of touch. Carolyn contributed to studies about the application of force-feedback devices in learning environments for elementary school students. She earned a Master of Science degree in mechanical engineering in 2011.

Carolyn joined Stryker Orthopaedics in Mahwah, NJ, from 2012 until 2014, where she applied her mechanical engineering skills as a sustaining product project engineer for hip implants and instruments. She gained a deep appreciation for the hard work and diverse expertise required to bring surgical implants and instruments from the manufacturing floor to the operating room. She became fascinated with understanding physiology of the human body and wanted to learn more about how this knowledge could improve treatment methods for movement impairment after injury or disease.

In 2014, Carolyn became a graduate student at the Joint Department of Biomedical Engineering at University of North Carolina at Chapel Hill and North Carolina State University. Her graduate work is part of a broader, long-term goal to understand the complex interactions

between bone and the neuromuscular system. Using a rat model of neonatal brachial plexus injury (NBPI), she has examined whether microarchitecture and mineralization of the shoulder (i.e., glenohumeral) joint is affected as has been seen in other clinical models of injury and disease that alter joint loading. Carolyn will continue to make small, but meaningful, contributions to biomedical research and hopes to help others do the same.

## ACKNOWLEDGMENTS

This study would not have been possible without generous contributions from the following talented individuals:

To Jacque and Kate – Thank you both for supporting me over the past three years. I am grateful for your time, the opportunities you made available to me, and the encouragement you have given me during a season of life that has seen milestone transitions and personal growth. I am proud to have been part of the Orthopaedic Mechanobiology Laboratory and Movement Biomechanics Laboratory.

To Greg – Thank you for offering your time, valuable insight, and serving on my committee. I particularly admire how you share your passion for rehabilitation engineering with your students and colleagues. Best wishes for assured continued success at Georgia Tech.

To Dustin – I am so glad that your postdoctoral work brought you back to NCSU. Your abilities as a researcher, technical writer, and creative artist continue to impress! Thank you for your kindness through e-mails, training sessions, and lunch talks. I am certain you will uncover great opportunities at The University of Tennessee, Knoxville.

To OMLers and MoBLers – Working with you has been a privilege! I am thankful for your generous contributions to this study and the ongoing research, thoughtful discussions, and your encouragement. Special thanks to Jon (and Nikki!) Doering and Nicholas Hanne for your friendship – you will persevere!

To Ted Bateman and Eric Livingston – Many thanks for support from the Bateman Lab. This work would not be possible without use of the SCANCO micro-computed tomography scanner and software. Special thanks to Eric for your troubleshooting talents and time – you are all-around great!

To the wonderful undergraduate students who contributed to this study and the ongoing NBPI research – Austin Murray (2015-2016 Abrams Scholar), Sophie Tushak (2016-2017 Abrams Scholar), Curtis Hudson, Amir Robe, Jennifer Antoniono, Maggie Tamburro, Hannah Thornburg, and Eric Warren – thank you for your hard work!

Funding was provided by the Orthopaedic Research and Education Foundation/Pediatric Orthopaedic Society of North America (KRS), Research Innovation Seed Funding from North Carolina State University (KRS, JHC), a Seed Grant from the Rehabilitation Engineering Core at the University of North Carolina and North Carolina State University (KRS, JHC), and R21 funding (R21HD088893) from the National Institutes of Health (KRS, JHC).

**TABLE OF CONTENTS**

## LIST OF TABLES

## LIST OF FIGURES

# CHAPTER 1: INTRODUCTION

## 1.1 Neonatal Brachial Plexus Injury Overview

Neonatal brachial plexus injury (NBPI) is the most common nerve injury in children (Abzug *et al*., 2015). Passing the infant's shoulders through the birth canal may require additional traction, and subsequently stretch or damage one or more of the cervical (C5-C8) or thoracic (T1) nerve roots that form the brachial plexus. Impaired arm movement follows depending on the severity of peripheral nerve injury and corresponding muscle denervation. Despite full neurologic recovery in 80-90% of cases, 30-40% of neonates sustain lifelong impairment in the affected arm (Abzug *et al*., 2015). Secondary musculoskeletal deformities, including gross morphologic changes to the humerus and the glenoid fossa of the scapula, persist even after spontaneous nerve recovery and are the most common reasons for surgical intervention post-injury (Abzug *et al*., 2015). Altered glenohumeral (GH) joint loading has been examined as the impetus for abnormal bone growth and development in these children, because mechanical forces impose necessary and critical stimuli for healthy skeletal growth and development (Frost, 1994). The regions in the GH joint that experience abnormal growth and morphological deformities are comprised primarily of cancellous bone, which is integral to the transfer of joint loading along the bone and is known to adapt to altered loads (Wolff, 1892/1986; Frost, 1994). However, the impact of the brachial plexus injury on this underlying cancellous bone is not well understood. This thesis examined whether underlying trabecular microarchitecture and mineralization within the articulating bones at the injured GH joint were affected following NBPI. Characterizing post-injury properties of the underlying cancellous bone in the shoulder joint will provide critical and novel insight for improving rehabilitative

and regenerative therapies that preserve maximal limb function, especially given our current understanding of overall gross musculoskeletal deformities during postnatal development.

## 1.2 Relevant Shoulder Anatomy and Development

The shoulder is composed of the articulation of the humerus, scapula, and clavicle, with the primary joint being the glenohumeral joint articulation between the humeral head and the glenoid fossa of the scapula. The joint is actuated by the GH muscles which enable humeral elevation and rotation. Muscles of the upper limb are innervated by cervical and thoracic nerve roots C5-T1 by way of the brachial plexus. Details of these structures and the development of the humerus and scapula are described below.

### 1.2.1 Humerus Development

The humerus, a long bone that undergoes endochondral ossification (Figure 1.1), is one of the two bones involved in GH joint development. During endochondral ossification, mesenchymal stem cells (MSCs) condense and differentiate into chondrocytes, which collectively form a cartilaginous template, or anlage. The chondrocytes mature and become hypertrophic. The historical view was that these hypertrophic chondrocytes underwent apoptosis, and vasculature then invaded the anlage, bringing osteoblast progenitors to replace that cartilage with bone (Berendsen & Olsen, 2015). However, recent evidence suggests that the hypertrophic chondrocytes can transdifferentiate into osteoblasts directly (Yang, Tsang, Tang, Chan, & Cheah, 2014; Zhou, Yue, Murphy, Peyer, & Morrison, 2014). Either way, the middle of the anlage, commonly referred to as the bone collar, becomes the site of the primary ossification center. One or more secondary ossification centers appear in the humerus between

ages 0 and 4 years in the non-ossified cartilaginous epiphysis (Kwong, Kothary, & Poncinelli, 2014). Between 4 and 10 months of age, a secondary ossification center forms in the medial half of the humeral head. Another secondary ossification center forms to become the greater tubercle after age 10 months. These secondary ossification centers fuse together in an anteroposterior direction; between ages 5 and 9 years, they continue to fuse, extending to the region that will become the lesser tubercle (Kwong *et al*., 2014).

The proximal humeral growth plate is partially closed between 14 and 16 years of age, with the posterolateral region as the last portion to close, according to clinical magnetic resonance imaging (MRI) studies (Kwong *et al.*, 2014). Complete ossification of the proximal humerus occurs between ages 13 and 17 years.

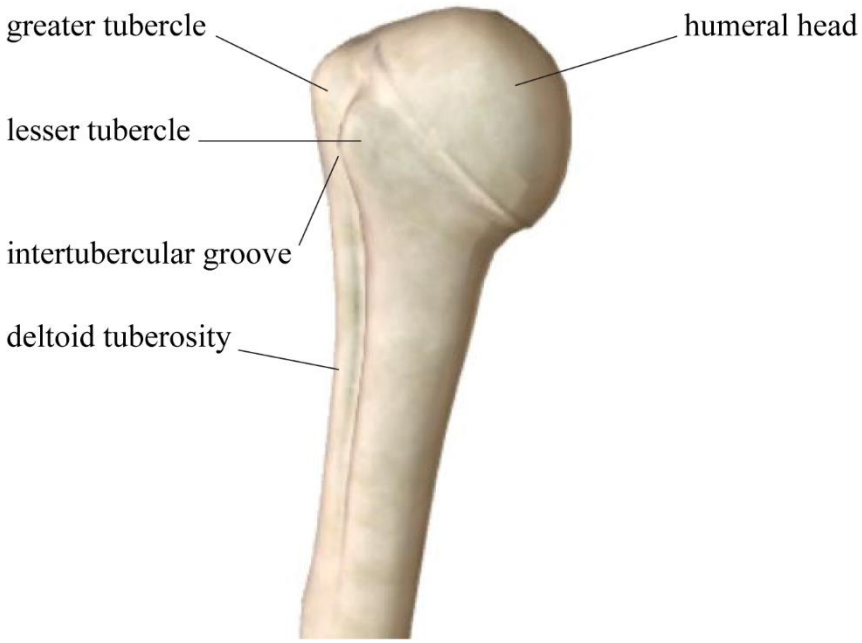


**Figure 1.1 Right proximal humerus, anterior view. Landmark features at skeletal maturity are marked (Moore & Dalley, 1999; adapted from https://human.biodigital.com/).**

### 1.2.2 Scapula Development

The scapula, which is the other bone involved in GH joint development, is a unique flat bone that undergoes both endochondral and intramembranous ossification (Iannotti, 2007; Rockwood & Matsen, 2009) (Figure 1.2). During intramembranous ossification, MSCs directly differentiate into osteoblasts such that a cartilaginous template is not needed to begin depositing mineralized bone matrix (Berendsen & Olsen, 2015). The scapula is formed from seven or more primary and secondary ossification centers (Kothary, Rosenberg, Poncinelli, & Kwong, 2014). The body and spine of the scapula are formed via intramembranous ossification and are ossified at birth (Bain, Itoi, Di Giacomo, & Sugaya, 2015).

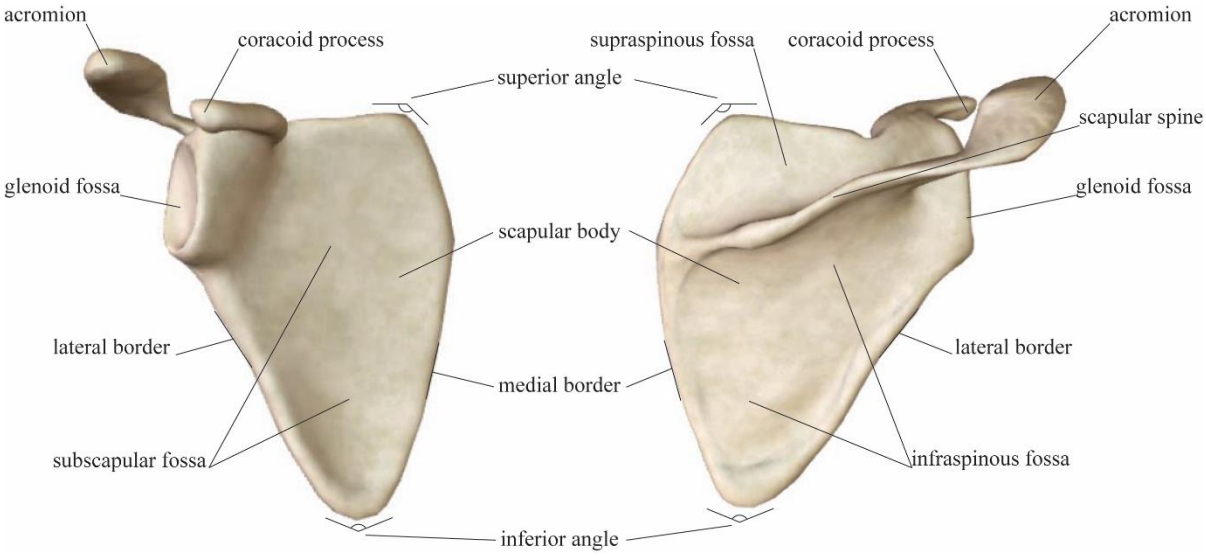


**Figure 1.2 Right scapula, anterior (left) and posterior (right) views (Moore & Dalley, 1999; adapted from https://human.biodigital.com/).**

The primary ossification center forms the body of the scapula at birth, while the distal glenoid is cartilaginous (Kothary *et al*., 2014). Likewise, the coracoid primary ossification center appears at birth or within the first few months postnatally (Ogden & Phillips, 1983). At

2 years of age, a bipolar growth plate forms between the scapula and coracoid primary ossification centers, extending into the non-ossified region of the superior glenoid. The distal acromion is a primary ossification center that advances anteriorly toward the acromioclavicular joint (Zember, Rosenberg, Kwong, Kothary, & Bedoya, 2015).

The first secondary ossification center is formed within the subcoracoid region between 8 and 10 years of age and forms the upper-third of the glenoid articular surface once ossified. Fusion of this secondary ossification center begins between ages 14 and 15 years and completes between ages 16 and 17 years, connecting the coracoid with the scapula. Another secondary ossification center forms the inferior two-thirds of the glenoid, appearing as islands around the periphery of the glenoid (Kothary *et al.*, 2014). They merge as a horseshoe-shaped epiphysis and fuse with the glenoid rim and subcoracoid secondary ossification center. The cartilaginous precursor forming the glenoid first appears concave, while the subchondral bony plate is slightly convex to flat. Between ages 10 and 11 years, the ossified glenoid adopts a concave conformation (Ogden & Phillips, 1983). Bone growth expands toward the glenoid center and completely fuses between 17 and 18 years of age (Kothary *et al*., 2014).

### 1.2.3 Scapulohumeral Muscles

NBPI causes damage to one or more of the nerve roots that innervate muscles which cross the humerus, scapula, or both. The supraspinatus, infraspinatus, teres minor, and subscapularis are muscles innervated by cervical nerve roots within the brachial plexus and attach to both the humerus and scapula (Table 1.1). Collectively, this group comprises the rotator cuff muscles, which are primarily responsible for stabilizing the humeral head within the glenoid fossa during joint movement. Other muscles that attach to either the humerus or

scapula include the teres major, deltoid, biceps brachii (i.e., long and short heads), brachialis, and coracobrachialis (Table 1.1). Like the rotator cuff muscles, these muscles are innervated by the cervical roots in the brachial plexus. Primary innervation is supplied by the subscapular, axillary, and musculocutaneous nerves.

**Table 1.1 RC muscles crossing the glenohumeral joint with primary innervation in bold (Moore & Dalley, 1999).**

| Muscle | Proximal Attachment | Distal Attachment | Innervation | Main Action |
|---|---|---|---|---|
| Supraspinatus | Supraspinous fossa of scapula | Superior facet on greater tubercle of humerus | Suprascapular nerve (**C5** and C6) | Abducts arm with assistance from deltoid |
| Infraspinatus | Infraspinous fossa of scapula | Middle facet on greater tubercle of humerus | Suprascapular nerve (**C5** and C6) | Rotates arm laterally |
| Teres minor | Superior part of lateral border of scapula | Inferior facet on greater tubercle of humerus | Axillary nerve (**C5** and C6) | Rotates arm laterally |
| Teres major | Dorsal surface of inferior angle of the scapula | Medial lip of intertubercular groove of humerus | Lower subscapular nerve (**C6** and C7) | Rotates arm medially and adducts it |
| Subscapularis | Subscapular fossa | Lesser tubercle of humerus | Upper and lower subscapular nerves (C5, **C6**, and C7) | Rotates arm medially and adducts it |
| Deltoid (3 compartments) | Lateral third of clavicle, acromion, and spine of scapula | Deltoid tuberosity of humerus | Axillary nerve (**C5** and C6) | Anterior: flexes and medially rotates arm<br>Middle: abducts arm<br>Posterior: extends and laterally rotates arm |
| Biceps brachii (2 heads) | Short head: tip of coracoid process of scapula<br>Long head: supraglenoid tubercle of scapula | Tuberosity of radius and fascia of forearm via bicipital aponeurosis | Musculocutaneous nerve (C5 and **C6**) | Supinates forearm and flexes forearm in the supine position |
| Brachialis | Distal half of anterior surface of humerus | Coronoid process and tuberosity of ulna | Musculocutaneous nerve (C5 and **C6**) | Flexes forearm in all positions |
| Coracobrachialis | Tip of coracoid process of scapula | Middle third of medial surface of humerus | Musculocutaneous nerve (C5, **C6**, C7) | Assists to flex and adduct arm |

## 1.3 Effects of NBPI on the Shoulder

### 1.3.1 Musculoskeletal Effects and Functional Implications of NBPI in the GH Joint

Glenohumeral deformities that develop secondary to NBPI are the most common reasons for surgical intervention post-injury to improve passive and active range of motion in the shoulder (Abzug *et al*., 2015). Secondary skeletal dysplasia, or abnormal bone growth, is present in both the humerus and the scapula. Skeletal dysplasia in the humerus and scapula has been observed in many MRI studies (Pearl *et al.*, 2003; van Gelein Vitringa, van Kooten, Mullender, van Doorn-Loogman, & van der Slujis, 2009; Clarke, Chafetz, & Kozin, 2010). Osseous deformities in the humerus include flattening of the articulating humeral head (HH) (Reading *et al*., 2012), decreased HH diameter, and posterior and inferior subluxation. Studies by McDaid *et al*. and Bain *et al.* have observed shorter arm length on the observed side (Bain, DeMatteo, Gjertsen, Packham, Galea, & Harper, 2012). The involved limb was shorter than the uninvolved limb (average of 92% of uninvolved limb), in which the humeral length averaged 93% and the forearm length averaged 90% of the uninvolved limb length (McDaid, Kozin, Thoder, & Porter, 2002). Most scapular deformities are seen in the glenoid fossa, including glenoid retroversion, declination, loss of glenoid concavity, and pseudoglenoid formation (Abzug *et al.*, 2015). Glenoid retroversion and less declination are present, and findings from the 3D MRI studies have concluded that GH dysplasia not only exists in the axial plane but extends to other planes as well (Eismann, Laor, & Cornwall, 2016). In a study by Sibinski *et al.*, older children were statistically more retroverted and had smaller HH size and deformed shape (Sibinski, Woźniakowski, Drobniewski, & Synder, 2010). Other scapular changes include smaller coracoid angle on the involved side, as well as retroversion of the glenoid and coracoid after injury (Soldado & Kozin, 2005).

Functional and postural sequelae have also been observed in concert with both skeletal and muscle changes. Waters *et al.* described posterior subluxation of the HH and increased retroversion, with an associated reduced Mallet score (Waters, Smith, & Jaramillo, 1998), a commonly used measure of upper limb function post-injury (Mallet, 1972). In a study by Eismann *et al.*, posterior HH translation was seen, but not outside the glenoid labrum, which was posteriorly elongated (Eismann *et al.*, 2016). In a study by van Gelein Vitringa *et al.*, increased glenoid retroversion and posterior HH subluxation was observed in conjunction with smaller muscle size on the affected side compared to the contralateral (subscapularis 51%, infraspinatus 61%, and deltoid 76%) (van Gelein Vitringa *et al.*, 2009). They found that glenoid form was related to infraspinatus muscle atrophy and HH subluxation was related to infraspinatus and subscapularis atrophy. In this case, they did not see a correlation between atrophy and passive external rotation, nor to Mallet score. However, postural deformities are frequently observed, including shoulder internal rotation and elbow flexion contractures. Shoulder contracture has been associated with progressive skeletal dysplasia of the GH joint (Waters *et al.*, 1998).

### 1.3.2 NBPI Murine Models

Several mouse and rat models have been used to examine musculoskeletal changes following NBPI. Rat models show anatomical similarities at the shoulder joint when compared to humans, including presence of the rotator cuff muscles and skeletal features like the acromion and coracoid process on the scapula (Norlin, Hoe-Hansen, Oquist, & Hildebrand, 1994; Soslowsky, Carpenter, DeBano, Banerji, & Moalli, 1996). The advantage of using an animal model is that it captures *in vivo* joint changes in physiologically relevant ways that are

not yet fully realized or readily available in computational models. Likewise, murine models exhibit rapid development to reach musculoskeletal maturity, where 1 human year is equivalent to 2.6 days in a mouse (Dutta & Sengupta, 2016) and 10.5 days in a rat (Quinn, 2005). Murine models provide a relevant, feasible means to perform musculoskeletal research that pertains to the glenohumeral joint.

NBPI has been replicated in murine models using a variety of interventional approaches to understand the development of GH osseous and postural deformities. One mouse model used intramuscular injections of botulinum toxin A (Botox) to paralyze the supraspinatus in mice at birth, due to this muscle's superficial location beneath the skin and its ability to replicate muscle weakness commonly observed in NBPI infants (Kim, Galatz, Patel, Das, & Thomopoulos, 2009; Potter, Havlioglu, & Thomopoulos, 2014). Kim *et al.* performed subsequent injections over 2, 4, 8, 12, and 16 weeks to maintain paralysis, while other mice were allowed to recover at these timepoints (14, 12, 8, 4, and 0 weeks recovered, respectively). The contralateral shoulder was injected with an equivalent dose of saline for all three groups: Botox (i.e., NBPI model), recovery, and normal (i.e., control). The authors hypothesized that the NBPI mouse model would show similar GH deformities to the clinical condition. They also predicted that longer periods of muscle paralysis would worsen deformities, while longer periods of recovery would alleviate deformities. Muscles that cross the scapula, such as the supraspinatus, infraspinatus, teres minor, and posterior deltoid were visibly atrophic. Supraspinatus muscle volume grew at a significantly slower rate in Botox-injected shoulders than the saline-injected and normal shoulders. Botox-injected shoulders also exhibited significantly smaller mean GH abduction (61.7° ± 8.1°) and passive elbow extension angles (114.9° ± 5.0°) when compared to contralateral, saline-injected (abduction: 125.8° ± 7.7°;

extension: 155.8° ± 1.7°) and normal shoulders (abduction: 122.6° ± 6.3°; extension: 151.8° ± 5.9°). Humeral head bone volume and trabecular thickness were significantly lower in the NBPI model compared to contralateral and normal shoulders. Likewise, trabecular number and separation significantly increased with respect to longer periods of chemodenervation. Overall length and diaphyseal diameter of the humerus and glenoid surface area in the scapula were significantly smaller in the NBPI model with respect to contralateral and normal shoulders. Interestingly, the Botox-injected shoulders showed larger relative humeral anteversion and decreased glenoid version. Using Botox to induce paralytic effects consistent with NBPI, Kim *et al.* provided evidence that microstructural changes, at least in the humerus, may be concurrent with global changes in muscle architecture and GH joint morphology. However, Botox may cause weakness in muscles that are adjacent to the injected target muscles (Yaraskavitch, Leonard, & Herzog, 2008), and it may have systemic effects that impact muscle or bone development separate from nerve effects. Predicting the extent and rate at which Botox diffuses into surrounding muscle tissue may be difficult to control, and thus chemodenervation with Botox may not be an ideal NBPI model.

Other murine models have directly replicated nerve injury via neurectomy surgery, which involves directly severing nerve roots (Li *et al*., 2008; Nikolaou, Peterson, Kim, Wylie, & Cornwall, 2011). In a rat model of NBPI, Li *et al*. performed a right-side C5-C6 root neurectomy in 5-day-old Sprague Dawley rats, while the left shoulder served as a contralateral control. Significant shoulder internal rotation contracture occurred within 4 weeks after surgery, in which passive mean external rotation was 116° ± 10° for the affected shoulder and 167° ± 7° for the contralateral shoulder. Glenoid version was 8° ± 3° of anteversion on the affected side and 2° ± 2° of retroversion on the contralateral side. For six specimens, histologic

examinations revealed visibly smaller humeral head size on the affected side when compared to the contralateral side. The GH joint exhibited dysplastic articulating geometry, in which four glenoids showed thicker articular cartilage and abnormal fossa features (i.e., biconcave, flatter), while two humeri showed flatter humeral head geometry. A study by Crouch *et al*. examined the NBPI rat model and discovered that optimal muscle fiber length was significantly correlated with at least one osseous deformity, for six out of fourteen muscles, which suggests that altered muscle loading may affect overall joint development (Crouch *et al*., 2015). NBPI rat models, especially those that employ direct injury to the brachial plexus, are successful in their ability to recapitulate the clinical manifestations of shoulder deformity presented in humans.

### 1.3.3 NBPI Computational Models

Computational musculoskeletal modeling tools, such as OpenSim (Delp *et al.*, 2007), offer context for etiological joint changes that follow injuries like NBPI. Specifically, muscle parameters of the model that directly relate to the muscle's force-generating capacity, such as optimal fiber length, can be scaled based on reported evidence of pathologically shortened muscle in patients or animal models following injury. Likewise, muscle activation can be scaled in proportion to the muscle's full activation to simulate reported findings of muscle paresis or paralysis post-injury. The resultant musculoskeletal model captures these relative changes in muscle force-generating capacity, from which mechanistic explanations of joint deformity or altered limb movement can be deduced. As parametric representations of an injured joint, computational musculoskeletal models provide a deterministic way to think about

underlying mechanisms of deformity, despite current open questions concerning mechanobiological aspects.

Using an upper limb musculoskeletal model, Crouch *et al.* performed a computational sensitivity analysis to understand how shoulder muscles affected by NBPI were mechanically capable of producing osseous or postural deformities consistent with clinical findings (Crouch, Plate, Li, & Saul, 2014). Two posited mechanisms responsible for osseous and postural deformities defined muscle parameters in the model: the first was impaired longitudinal growth of paralyzed shoulder muscles, and the second, strength imbalance, in which intact internal rotator cuff muscles act unopposed to paralyzed external rotator cuff muscles. Affected muscles for the impaired growth condition were assigned muscle fiber lengths that were 30% shorter than optimal fiber length. For strength imbalance, muscles were assigned activations that were 30% of their full activation. The authors hypothesized that muscles crossing the posterior aspect of the shoulder were mechanically capable of contributing to osseous deformity, while muscles responsible for internal rotation and adduction of the shoulder were mechanically capable of contributing to postural deformity. Each deformity mechanism (i.e., impaired longitudinal growth or strength imbalance) was iteratively applied to each muscle, while all other muscles crossing the shoulder joint were inactive and could generate passive forces only. From the impaired growth mechanism, the subscapularis, infraspinatus, long head of the biceps, and long head of the triceps were capable of increasing posteriorly directed joint force. From strength imbalance, the subscapularis, infraspinatus, long head of the biceps, latissimus dorsi, teres major, teres minor, and posterior deltoid were capable of increasing posteriorly directed joint force. Shoulder external range of motion (ROM) was evaluated using simulated clinical examinations. From impaired growth, the anterior deltoid and subscapularis

reduced external shoulder rotation ROM by 52° and 40°, respectively, while the long head of the triceps reduced shoulder abduction by 56°. Shoulder external rotation ROM decreased by more than 10° via the strength imbalance mechanism for the subscapularis, anterior deltoid, and pectoralis major. The muscles identified as potential contributors to osseous or postural deformity from these simulations provide meaningful context to the present study (Chapter 2), in which changes in GH microstructure may be localized to regions near affected muscles that cross the GH joint.

A follow-up simulation study expanded the findings from the sensitivity analysis to observe impaired longitudinal growth, strength imbalance, and the combined effects of these mechanisms when applied to multiple muscles that may be affected by NBPI (Cheng, Cornwall, Crouch, Li, & Saul, 2015). Each of the three mechanisms (i.e., impaired longitudinal growth, strength imbalance, and their combined effects) was applied to all muscles affected by NBPI at the C5-6 level to observe the extent to which each mechanism contributed to osseous or postural deformity. The upper limb musculoskeletal model performed passive axial shoulder rotation with the elbow flexed to 90°. All mechanisms increased posteriorly directed, compressive GH joint forces and restricted axial shoulder rotation ROM when compared to an uninjured model. The impaired growth and combined mechanisms resulted in greater effects on posteriorly directed, compressive GH forces and external shoulder rotation ROM compared to strength imbalance alone. These findings highlight that pathologically shortened muscles may largely contribute to osseous and postural deformities, perhaps more so than denervated muscles that retain their length properties.

## 1.4 Effects of Mechanical Loading on Bone

Mechanical loading is critical for healthy skeletal development and maintenance throughout an individual's lifespan (Frost, 1994; Turner, 1998). Muscle contractions and inertial forces imposed by gravity are examples of external loads on the appendicular skeleton that are necessary to establish the expected mechanical loading environment. The resulting bone stresses and strains influence bone's response to mechanical loading, the *mechanobiological response*, in the bone-forming osteoblasts and bone-resorbing osteoclasts, which orchestrate bone remodeling (Mullender, Huiskes, & Weinans, 1994; Huiskes, Ruimerman, van Lenthe, & Janssen, 2000). These mechanobiological responses affect both cortical and cancellous bone and occur throughout life from development and growth to adult homeostasis.

Altered glenohumeral joint loading following NBPI may greatly influence underlying trabecular bone density and microstructure. Bone remodeling occurs in response to mechanical loading cues (Wolff, 1892/1986; Roux, 1895; Frost, 1994). Trabecular microstructure has been studied broadly to understand the load-bearing characteristics of bone (Anderson *et al*., 2016; Keaveny, Morgan, Niebur, & Yeh, 2001), and trabecular bone loss has been observed in a variety of clinical scenarios with altered mechanical loading. Spaceflight resulted in decreased bone mineral density (BMD) in the tibia (Vico *et al*., 2000), spine, and hip (Lang *et al*., 2004). Prolonged bedrest induced increased trabecular number (Tb.N) and decreased trabecular thickness (Tb.Th) and separation (Tb.Sp) in the distal tibia following prolonged bedrest (Kazakia *et al*., 2014). Spinal cord injury led to decreased BMD in the femoral and tibial epiphyses (Eser *et al*., 2004). In a mouse model, NBPI was associated with altered Tb.N and Tb.Sp in the humeral epiphysis (Kim *et al*., 2010; Potter *et al*., 2014). Such findings suggest

that trabecular density and microarchitecture may be affected following peripheral nerve injury, although they have not yet been fully characterized in all trabecular bone regions surrounding the GH joint.

### 1.4.1 Bone Microarchitecture

Withstanding load is one of the primary functions of bone. In the long bones of the appendicular skeleton, loads experienced during daily activities are transferred across the articular surface of joints through the underlying cancellous bone of the epiphysis and metaphysis and into the cortical bone of the diaphysis. The trabecular bone tissue adapts to these loads (Frost, 1994; Turner, 1998), resulting in changes to one or more of the standard metrics of bone density and microarchitecture: BMD, tissue mineral density (TMD), bone volume fraction (BV/TV), Tb.N, Tb.Th, and Tb.Sp and their standard deviations (Tb.Th.SD, Tb.Sp.SD) using direct 3D methods, connectivity density (Conn.D), structure model index (SMI), and degree of anisotropy (DA) (Table 1.2) (Bouxsein *et al*., 2010).

Trabecular density and microarchitecture, which can be characterized using micro-computed tomography (micro-CT), are important factors contributing to bone strength and thus the load bearing ability of bones (van der Meulen, Jepsen, & Mikić, 2001). The formation and maintenance of trabecular structure are determined by the activity of osteoblasts and osteoclasts. These cells, which dynamically regulate bone remodeling processes, are sensitive to changes in metabolism and mechanical loading. Therefore, trabecular bone properties are likely altered by NBPI, and understanding more about how this injury influences the underlying bone metabolism and structure may inform more effective treatment strategies to mitigate skeletal deformities following nerve injury.

**Table 1.2 Common metrics of trabecular bone (Bouxsein *et al*., 2010)**

| Metric | Description |
|---|---|
| Bone mineral density (BMD, $mg/cm^3$) | Bone mass per total volume |
| Tissue mineral density (TMD, $mg/cm^3$) | Bone mass per bone volume |
| Bone volume fraction (BV/TV, %) | Bone volume per total volume of interest |
| Trabecular number (Tb.N, $mm^{-1}$) | Mean number of trabeculae per unit length |
| Trabecular thickness (Tb.Th, mm) | Mean thickness of trabeculae |
| Trabecular separation (Tb.Sp, mm) | Mean distance between trabeculae |
| Trabecular thickness standard deviation (Tb.Th.SD, mm) | Homogeneity of trabecular thickness |
| Trabecular separation standard deviation (Tb.Sp.SD, mm) | Homogeneity of trabecular separation |
| Connectivity density (Conn.D, $mm^{-3}$) | Degree of connectivity of trabeculae normalized by total volume |
| Structure model index (SMI) | Indicator of the structure of trabeculae |
| Degree of anisotropy (DA) | Length of longest divided by shortest mean intercept length vector (i.e., measurement of structural anisotropy) |

### 1.4.2 Mechanical Loading Effects on the Developing Skeleton

Mechanical stimuli via muscle contractions are important even at the embryonic stages of skeletal development. In two mouse models that cause reduced (Kassar-Duchossoy *et al*., 2004) or absent (Tajbakhsh, Rocancourt, Cossu, & Buckingham, 1997) skeletal muscle development, ossification centers of the humerus and scapula showed abnormal morphology or reduced bone formation in 'muscleless' limbs (Nowlan *et al*., 2010). Specific altered forelimb attributes included significantly irregular calcification in the humeral mid-diaphysis and a smaller humeral deltoid tuberosity in 'muscleless' limbs, delayed calcification in the scapular blade of reduced muscle limbs, and decreased humeral and scapular total length in both 'muscleless' and reduced limbs (Nowlan *et al*., 2010). Altered mechanical loading has also led to gross morphological deformities, such as large neck-shaft and anteversion angles in the proximal femur and a shallow acetabulum seen in developmental hip dysplasia (Laplaza, Root, Tassanawipas, & Glasser, 1993; Shefelbine & Carter, 2004).

### 1.4.3 Mechanical Loading Effects on the Adult Skeleton

Even in developed bone, bone loss following decreased mechanical loading is well established. Both gross morphological features and underlying cancellous bone can be affected by abnormal loading scenarios, as evidenced by numerous studies in which reduced mechanical loading has resulted in trabecular bone loss. For example, decreased bone mineral density has been measured in the tibia, spine, and hip following spaceflight (Vico *et al*., 2000), increased trabecular number and decreased trabecular thickness and separation have been reported in the distal tibia following prolonged bedrest (Kazakia *et al*., 2014), and decreased bone mineral density has been noted in the femoral and tibial epiphyses following spinal cord

injury (Eser *et al*., 2004). ***We hypothesize that trabecular density and microarchitecture adapt similarly during postnatal development following NBPI, given the supporting evidence from other clinical scenarios and the remarkable skeletal dysplasia known to occur in clinical cases of NBPI.***

### 1.4.4 Thesis Overview

This thesis evaluates the hypothesis that neonatal brachial plexus injury alters trabecular bone properties. It is comprised of the following chapters:

*Chapter 2: Characterizing Trabecular Bone Properties Near the Glenohumeral Joint in a Rat Model of Neonatal Brachial Plexus Injury* (Coauthors: Austin F. Murray, Dustin L. Crouch, Katherine R. Saul, and Jacqueline H. Cole)

This chapter focuses on the study purpose, methods, results, discussion, and limitations. Carolyn McCormick performed micro-CT analyses, led data interpretation, and wrote the manuscript. Austin Murray contributed to micro-CT analyses, data interpretation, and manuscript writing. Dustin Crouch collected data used for this study and edited the manuscript. Jacqueline Cole and Katherine Saul developed the study, supervised data collection, analyses, and interpretation, and edited the manuscript.

*Chapter 3: Future Work*

This chapter discusses how the findings reported in this thesis can motivate and guide future research questions.

# CHAPTER 2: CHARACTERIZING TRABECULAR BONE PROPERTIES NEAR THE GLENOHUMERAL JOINT IN A RAT MODEL OF NEONATAL BRACHIAL PLEXUS INJURY

This work has been prepared for submission to the Journal of Bone and Mineral Research. Authors: **McCormick CM**, Murray AF, Crouch DL, Saul KR, and Cole JH

## 2.1 Introduction

Neonatal brachial plexus injury (NBPI) is the most common nerve injury in children, and 30-40% of affected children sustain impaired function in the affected arm throughout their lifespan (Abzug *et al*., 2015). Severe upper limb paresis following NBPI may result in reduced passive and active range of motion, including internal rotation contracture at the shoulder and/or flexion contracture at the elbow (Reading *et al.*, 2012). Limb movement and proper muscle forces generate mechanical loading, which is critical for healthy bone growth and maintenance in the developing skeleton (Frost, 1994; Turner, 1998). Post-injury changes in mechanical loading may lead to secondary musculoskeletal deformities, such as flattening of the humeral head (Hogendoorn, 2010) or abnormal curvature of the glenoid fossa (Hoeksma *et al*., 2003; Hogendoorn, van Overvest, Watt, Duijsens, & Nelissen, 2010). Consequently, such deformities may compromise movement and inhibit restoration of joint function, despite full neurologic recovery in 80-90% of affected children (Pearl, 2009). Abnormal musculoskeletal development at the shoulder joint is the most common reason for post-injury surgical intervention to improve functional outcomes (Abzug *et al*., 2015). Very little is understood about the effects of peripheral nerve injury on the parallel postnatal development

of muscle and bone. This current gap in understanding poses a challenge for clinicians who wish to implement a standard of care that prevents joint deformity and restores maximal function for children with NBPI throughout their lifetime (Kozin, 2010).

Global musculoskeletal changes in the glenohumeral (GH) joint have been studied extensively to understand how osseous and postural deformities manifest and subsequently compromise movement in children with NBPI. Clinical imaging studies have revealed structural changes in muscles crossing the GH joint, including atrophy in the subscapularis (i.e., internal rotator), infraspinatus (i.e., external rotator), deltoid (Hogendoorn *et al.*, 2010; van Gelein Vitringa *et al*., 2009), and supraspinatus (Hogendoorn *et al*., 2010). Reports of muscle degeneration have varied and at times, yielded conflicting information, yet all have suggested that muscle atrophy correlates with GH deformity in the affected shoulder (Hogendoorn *et al*., 2010; van Gelein Vitringa *et al*., 2009; Waters, Monica, Earp, Zurakowski, & Bae, 2009). The relationship between abnormal musculature and the development of shoulder deformity has also been examined mechanistically in a series of computational (Cheng *et al*., 2015; Crouch *et al*., 2014) and animal (Kim *et al.*, 2010; Li, Barnwell, Tan, Koman, & Smith, 2010; Nikolaou *et al.*, 2011; Weekley *et al.*, 2012; Potter *et al*., 2014; Nikolaou, Hu, & Cornwall, 2015; Crouch *et al.*, 2015) studies. In these studies, impaired longitudinal growth of denervated muscles, has been shown to contribute to postural deformities in a mouse model of NBPI (Nikolaou *et al*., 2011; Weekley *et al*., 2012), with a possible mechanism of increasing compressive joint forces and promoting abnormal bone growth. This experimental work is corroborated by musculoskeletal simulations of the upper extremity demonstrating that impaired growth and strength imbalance between intact internal and paralyzed or weakened external rotator muscles are both uniquely and synergistically

capable of increasing compressive, posteriorly directed GH joint forces and reducing external range of motion in the shoulder (Cheng *et al*., 2015; Crouch *et al*., 2014).

Altered GH joint loading following NBPI may greatly influence underlying trabecular bone density and microstructure. Bone remodeling occurs in response to mechanical loading cues (Wolff, 1892/1986; Roux, 1895; Frost, 1994). Trabecular microstructure has been studied broadly to understand the load-bearing characteristics of bone (Anderson *et al*., 2016; Keaveny *et al*., 2001), and trabecular bone loss has been observed in a variety of clinical scenarios with altered mechanical loading. Spaceflight resulted in decreased bone mineral density (BMD) in the tibia (Vico *et al*., 2000), spine, and hip (Lang *et al*., 2004). Prolonged bedrest induced increased trabecular number (Tb.N) and decreased trabecular thickness (Tb.Th) and separation (Tb.Sp) in the ultra-distal tibia following prolonged bedrest (Kazakia *et al*., 2014). Spinal cord injury led to decreased BMD in the femoral and tibial epiphyses (Eser *et al*., 2004). In a mouse model, NBPI was associated with decreased Tb.N and increased Tb.Sp. in the humeral epiphysis (Kim *et al*., 2010; Potter *et al*., 2014). Such findings suggest that trabecular density and microarchitecture are affected following peripheral nerve injury, although they have not yet been fully characterized in all trabecular bone regions surrounding the GH joint.

The purpose of this study was to examine trabecular bone properties near the articulating GH surfaces (i.e., humeral head and glenoid fossa) in a previously established rat model of NBPI (Li *et al.*, 2008; Crouch *et al.*, 2015). The rat shoulder joint has been identified as an excellent model of the human shoulder (Norlin, 1994), especially when investigating surrounding musculature (Soslowsky *et al*., 1996). Our hypothesis is that peripheral nerve injury not only leads to gross morphological joint deformities but also alters underlying trabecular bone density and microarchitecture in both the humerus and scapula. Assessing

trabecular microstructure in the proximal humerus and glenoid fossa of the scapula, the two articulating regions of the GH joint, will provide much-needed insight to understand the development of postural and osseous deformities following NBPI and the load-bearing functions of bone that are necessary for healthy postnatal development and maintenance. An in-depth understanding of the trabecular changes in the glenohumeral joint may inform preventative or corrective treatments for gross joint changes associated with secondary musculoskeletal deformities post-injury.

## 2.2 Methods

### 2.2.1 Study Design

The study described herein was performed using tissues obtained from a previous study (Crouch *et al*., 2015). All animal procedures were approved by the Institutional Animal Care and Use Committee at the Wake Forest School of Medicine. Sixteen Sprague-Dawley rat pups (Harlan Laboratories, Indianapolis, Indiana) were grouped according to surgical intervention implemented five days after birth: neurectomy and sham ($n$=8 each) (Figure 2.1).

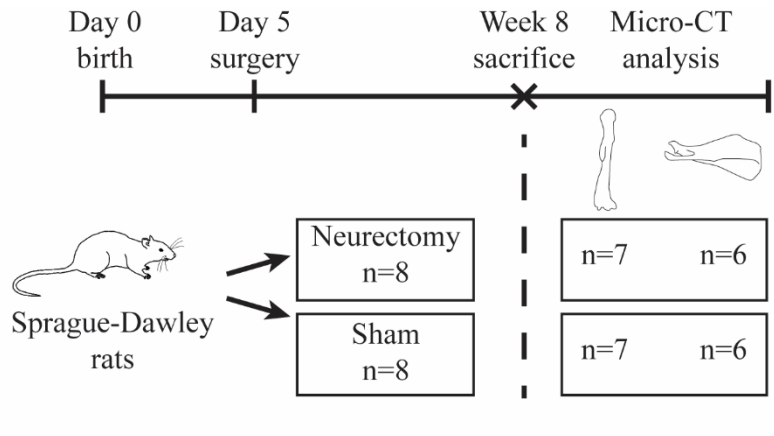


**Figure 2.1 Study design**

In the neurectomy group, NBPI was surgically induced in the left forelimb. Briefly, the rats were anesthetized with inhaled isoflurane, and a small transverse incision was made in the left pectoralis major muscle to expose the brachial plexus. The C5 and C6 nerve roots and the upper trunk of the brachial plexus were identified proximal to the origin of the suprascapular nerve and transected. The wound was irrigated with saline and closed with 6-0 nylon suture. Postoperatively, the rats were given butorphanol tartrate to manage pain. The sham group received a similar surgery in which the pectoralis major on the left side was incised, but the brachial plexus was left intact.

Eight weeks postoperatively, the rats were sacrificed, and the left (affected) and right (control) humeri and scapulae were excised. The bones were fixed in 10% neutral buffered formalin for forty-eight hours and subsequently immersed in 70% ethanol for storage. One humerus per group and two scapulae per group were damaged during the original dissection and thus were excluded from this study (Figure 2.1).

### 2.2.2 Micro-computed Tomography

Bone density and microarchitecture were assessed with quantitative micro-computed tomography (micro-CT). The bones were scanned at 45 kVp and 177 μA using a 0.5-mm Al filter (μCT 80, SCANCO Medical AG, Brüttisellen, Switzerland) and reconstructed at an isotropic voxel size of 10 μm. Density measurements were calibrated using the SCANCO hydroxyapatite calibration phantom, and a threshold of 441 mg/cm$^3$ (3891 Hounsfield units) was applied for bone.

For analysis, the humeri were manually reoriented such that the long axis of the bone was parallel to the z-axis. All humeri were manually positioned in the same x-y orientation for consistency. The scapulae were automatically reoriented with the scapular spine parallel to the z-axis and positioned in the same x-y orientation using SCANCO's 'fe_align' command. Cancellous bone volumes of interest (VOIs) were chosen near the glenohumeral joint, which was expected to be most affected following nerve injury. Using the contour and morphing tools in the SCANCO analysis software, two VOIs were selected in the proximal humerus (Figure 2.2a), and three VOIs were selected in the glenoid fossa region of the scapula (Figure 2.2b). All VOI lengths were chosen based on the maximum possible length in a given region for the smallest bone, and the VOIs do not include primary bone trabeculae near the growth plate.

The first humeral VOI was 12.5% of the total humeral length and was defined in the epiphysis, beginning inferior to the articular surface and extending distally toward the proximal growth plate. The second humeral VOI was 5% of the total humeral length and was defined in the metaphysis, beginning inferior to the proximal growth plate and extending distally toward the diaphysis. The three scapular VOIs were defined in secondary ossification centers formed during postnatal development (Kothary *et al.*, 2014). The first scapular VOI was 6.5% of the

total scapular length and was positioned in the subcoracoid secondary ossification center, beginning next to the articular surface and extending proximally along the scapular spine axis toward the superior glenoid physis. The second scapular VOI was 1.5% of the total scapular length and was defined in the upper region of the inferior glenoid secondary ossification center. It began on the inferior edge of the physis in the first VOI and extended proximally along the scapular spine. The third VOI was 7.5% of the total scapular length and was defined within the scapular neck, beginning next to the physis running across the width of the neck and extending proximally.

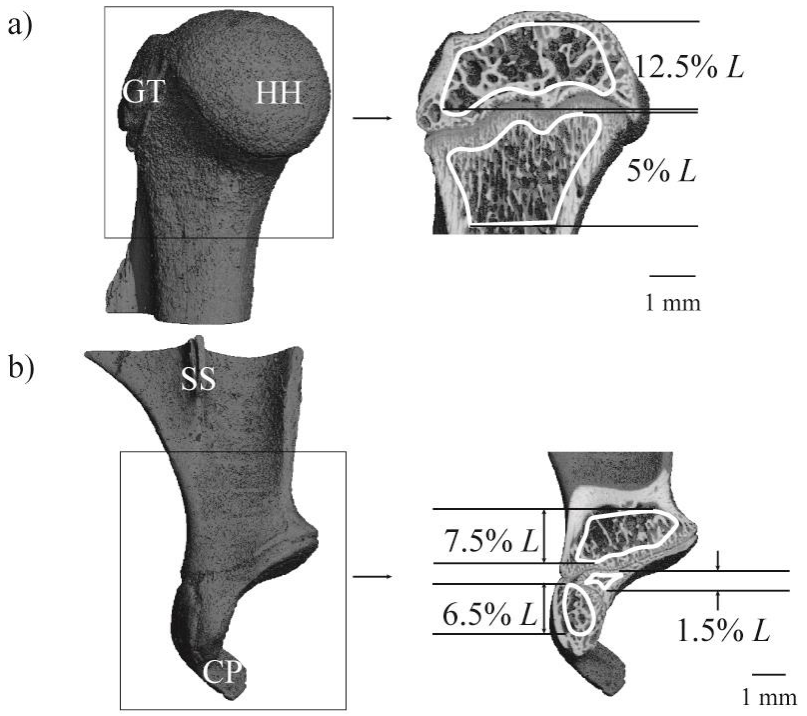


**Figure 2.2 VOIs for the humerus (a) and scapula (b) were chosen according to ossification centers, or zones.**

Each VOI was evaluated using the SCANCO analysis software to quantify bone mineral density (BMD), tissue mineral density (TMD), bone volume fraction (BV/TV), Tb.N, Tb.Th and Tb.Sp and their standard deviations (Tb.Th.SD, Tb.Sp.SD) using direct 3D

methods, connectivity density (Conn.D), structure model index (SMI), and degree of anisotropy (DA) (Bouxsein *et al*., 2010).

### 2.2.3 Statistical Analyses for Affected (Left) Side Comparisons

Differences in bone density and microarchitecture between the neurectomy and sham groups were examined using two-tailed unpaired t-tests with Welch's correction for unequal variances (Prism 6, GraphPad Software, Inc., La Jolla, CA). A significance level of 0.05 was used for all analyses. Trends between trabecular bone metrics in both groups were identified and defined as $p<0.8$.

Gross morphological metrics in the neurectomy shoulders (e.g., humeral head translation, glenoid inclination and version angles) were compared to trabecular bone metrics (e.g., density and microarchitecture) in the humerus and scapula. Specifically, two-tailed linear correlations were performed with respect to significant ($p<0.05$) or trending ($p<0.8$) differences in the GH joint, and either Pearson or Spearman correlation coefficients were computed, as appropriate (Prism 6, GraphPad Software, Inc., La Jolla, CA).

## 2.3 Results

### 2.3.1 Humerus Trabecular Bone

Trabecular bone microarchitecture and tissue mineralization were reduced in the proximal humerus of the neurectomy group relative to sham, and these differences were similar in the humeral epiphysis and metaphysis (Figure 2.3). Trabecular thickness tended to be 12% lower in the neurectomy group relative to sham ($p=0.076$ epiphysis, $p=0.057$ metaphysis). Trabecular TMD tended to be 4.2% lower in the neurectomy group compared to the sham group ($p=0.072$ epiphysis, $p=0.12$ metaphysis). The data for Tb.N, Tb.Sp, and BV/TV were more variable, and no significant differences were detected between groups.

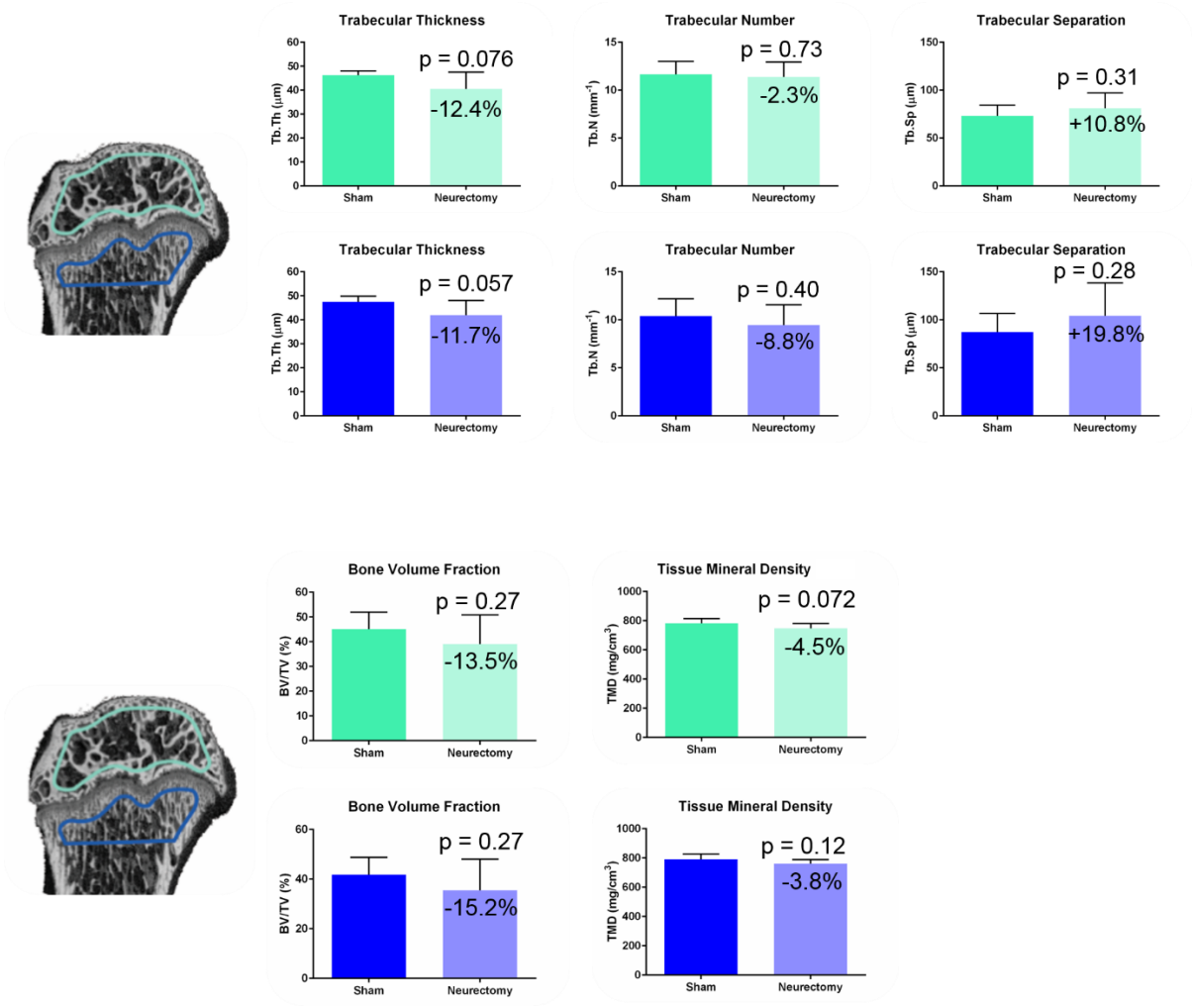


**Figure 2.3 The epiphyseal and metaphyseal regions of the humerus showed similar differences in trabecular bone microarchitecture between the neurectomy and sham groups.**

### 2.3.2 Scapula Trabecular Bone

Trabecular bone volume and microarchitecture in the glenoid fossa were different in the neurectomy and sham groups (Figure 2.4). Relative to sham, the neurectomy group had significantly lower BV/TV (-18.6% in zone 2, p=0.0027) and Tb.N (-17.5% in zone 3, p=0.011) and greater Tb.Sp (28.8% in zone 1, p=0.029 and 31.6% in zone 3, p=0.020). A trend

for reduced BV/TV was also observed in zone 3 (-13.4%) in the neurectomy group relative to sham (p=0.062).

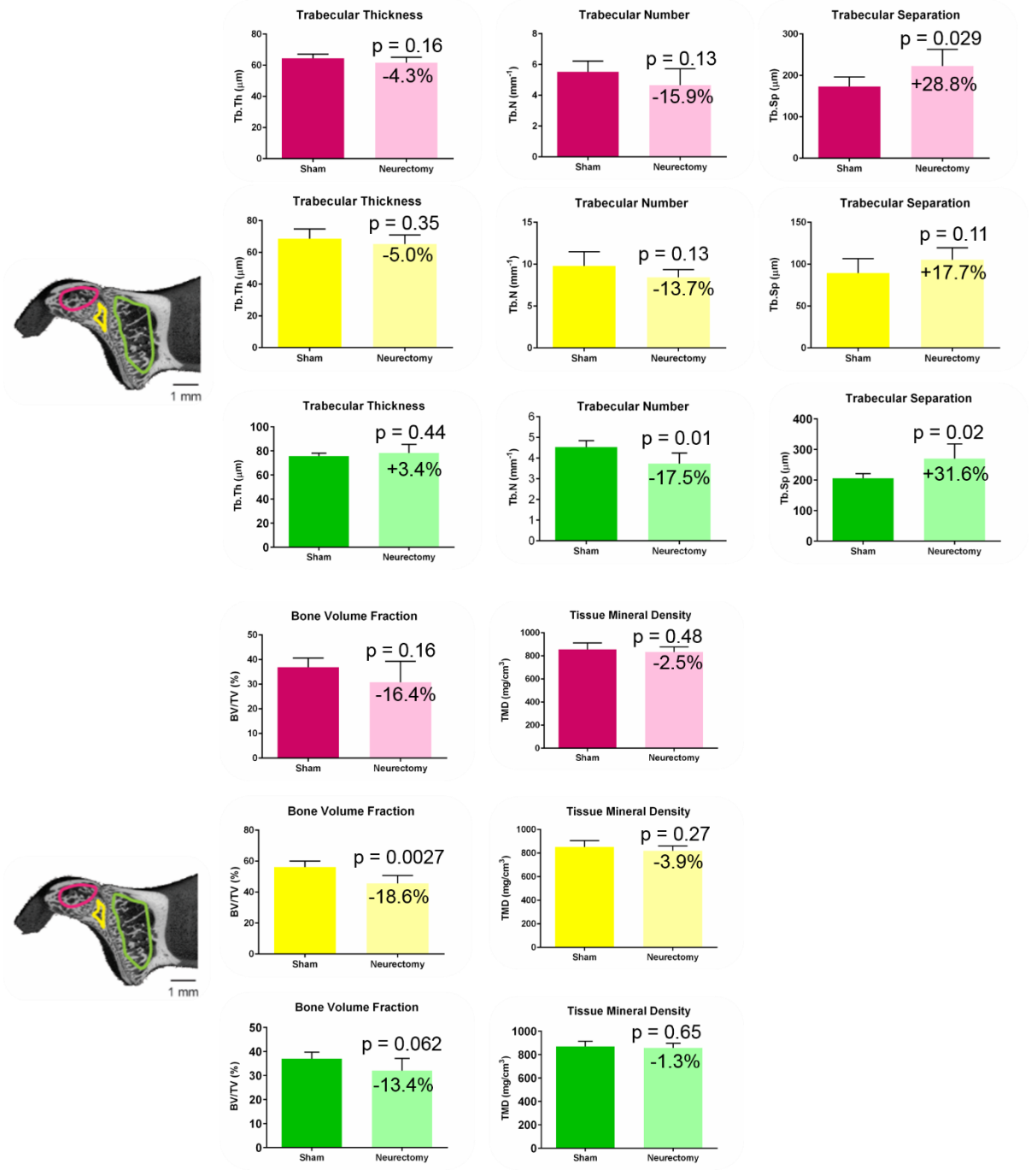


**Figure 2.4 All three scapular zones exhibited differences in trabecular microarchitecture for the neurectomy group compared with the sham group.**

### 2.3.3 Correlation Analysis between Bone Morphology and Trabecular Density and Microarchitecture

All morphological measurements in the neurectomy shoulders were linearly correlated with at least one trabecular bone metric. Glenoid inclination and humeral head superoinferior translation were strongly correlated with microarchitecture properties in both the humerus and scapula.

**Table 2.1 Pearson's correlation coefficients (r) and associated p-values for correlations of trabecular density and microarchitecture with gross bone morphology of NBPI rat shoulders. p<0.05 in bold.**

| | | | Bone Density and Microarchitecture | | | | | | | |
|---|---|---|---|---|---|---|---|---|---|---|
| | | | Scapula | | | | | Humerus | | |
| | | | Zone 1 | Zone 2 | Zone 3 | | | Epiphysis | | Metaphysis |
| | Morphology[a] | | Tb.Sp | BV/TV | BV/TV | Tb.N | Tb.Sp | Tb.Th | TMD | Tb.Th |
| Glenoid Fossa | Version | r | -0.47 | **0.17** | 0.41 | 0.44 | -0.39 | 0.42 | 0.51 | 0.45 |
| | | p | 0.12 | **0.030** | 0.17 | 0.16 | 0.21 | 0.18 | 0.094 | 0.14 |
| | Inclination | r | **-0.78** | **0.79** | **0.79** | **0.84** | **-0.87** | **0.86** | **0.59** | **0.82** |
| | | p | **0.0026** | **0.0024** | **0.0023** | **0.0006** | **0.0003** | **0.0004** | **0.045** | **0.0011** |
| Humeral Head | Anteroposterior Subluxation | r | 0.55 | **-0.62** | **-0.59** | -0.41 | 0.39 | -0.55 | -0.27 | **-0.59** |
| | | p | 0.064 | **0.031** | **0.042** | 0.19 | 0.22 | 0.063 | 0.40 | **0.043** |
| | Superoinferior Translation | r | **-0.71** | **0.77** | **0.89** | **0.79** | **-0.80** | **0.91** | **0.60** | **0.89** |
| | | p | **0.0093** | **0.0031** | **0.0001** | **0.0021** | **0.0019** | **<0.0001** | **0.0384** | **<0.0001** |

[a] For gross morphological measurements of the scapula and humerus, see Crouch *et al.*, 2015.

## 2.4 Discussion

The goal of this study was to investigate whether trabecular bone density and microarchitecture are altered in regions near the GH joint following neonatal brachial plexus injury in rats. Our findings show clear differences in trabecular bone properties in the neurectomy (i.e., NBPI) group relative to sham. The most profound changes in trabecular metrics occurred in the scapula. Scapulae in the neurectomy group demonstrated significant trabecular deficits relative to sham, including decreased BV/TV (zone 2) and Tb.N (zone 3) and increased Tb.Sp (zones 1 and 3). Humeri in the neurectomy group exhibited a tendency for reduced TMD in the epiphysis and thinner trabeculae (i.e., Tb.Th) in both the epiphysis and metaphysis. In addition to the gross morphological changes known to occur in the NBPI shoulder, our results suggest that NBPI compromises the underlying trabecular bone in regions near the articular surfaces of the glenohumeral joint.

Our trabecular bone findings align with other studies that have quantified trabecular microarchitecture following transient periods of muscle paralysis with nerve injury, chemodenervation with Botox, and spinal cord injury (SCI). Four weeks after neurectomy, CD-1 mice showed 22.2% reduced Tb.Th in the humeral epiphysis of affected shoulders compared to that of the contralateral limb and 17.7% compared to the sham group. After twelve weeks, Tb.Th reduced to 42.2% relative to the contralateral limb and 50% relative to sham (Kim *et al.*, 2010). Longitudinal imaging studies with our NBPI rat model may reveal increased disparities in affected shoulders compared to contralateral or sham shoulders, as shown in Kim *et al.* and other clinical studies (Waters *et al*., 1998; van der Slujis *et al*., 2001). In a model of transient paralysis, sixteen-week-old female C57B6J mice were injected with Botox in their hindlimbs. BV/TV was significantly reduced in the proximal tibial metaphysis within three

days (-25.5 ± 3.8%, $p<0.05$) and continued to the endpoint at twelve days (-76.8 ± 2.9%, $p<0.001$) (Poliachik, Bain, Threet, Huber, & Gross, 2010). Four weeks after spinal cord injury (SCI), induced in six-week-old male Sprague-Dawley rats, BV/TV was significantly reduced by 43% in the proximal tibial metaphysis for SCI rats compared with age-matched, intact controls (SCI: 6.78%, control: 15.6%) (Liu *et al.*, 2008). In our rats, we saw significantly reduced BV/TV in zone 2 of neurectomy scapulae (-18.6%, $p=0.0027$) after eight weeks. Our observed trabecular bone losses, in conjunction with other murine models of paralysis, suggest that NBPI can compromise bone development shortly after injury and more severely over time. Variable degradation of trabecular bone, as shown in these animal studies, suggests that timing of post-injury treatment is critical to bone health.

Knowledge about changes in localized regions of trabecular bone underlying the articulating surfaces of the GH joint brings additional context to the gross morphological changes observed in shoulders of NBPI patients. Compromised trabecular microstructure in the NBPI shoulder suggests that the load-bearing capacity may be reduced in the bones of the affected joint. Trabecular microarchitecture, including the size of individual trabeculae and their spatial distribution, is a major contributing factor to whole bone strength (Cole & van der Meulen, 2011).

Potential increases in fracture risk due to diminished physical properties of trabeculae (e.g., Tb.N, Tb.Th, or Tb.Sp) has been shown in other clinical cases like osteoporosis (Parfitt *et al.*, 1983) and osteopenia (Stein *et al.*, 2014). Altered trabecular bone microarchitecture is a strong indicator of fracture in other clinical cases. For example, reduced Tb.N is a significant predictor of vertebral fracture in middle-aged men diagnosed with osteopenia (Legrand *et al.*, 2000). The high proportion of children that spontaneously recover from NBPI may be at an

increased likelihood for fracture as they resume or increase activity levels, as this increased activity may increase loads on the affected bones to a threshold level that is above the bone load-bearing capacity. Our findings suggest that trabecular microarchitecture in NBPI shoulders are altered post-injury, with the potential outcome of decreased load-bearing capacity, and hence increased likelihood for fracture in later years.

Longitudinal studies observing NBPI patients into adulthood are needed to determine whether they have increased fracture risk. Currently, no studies have addressed monitoring long-term susceptibility to fracture in NBPI patients as they reach adulthood (i.e., skeletal maturity). Furthermore, changes in bone material properties, which also contribute to bone strength (van der Meulen *et al*., 2001), remain unknown for either animal models or clinical cases of NBPI. We found trends for small reductions in trabecular bone tissue mineral density (VOI means: -4.2% for humerus, -2.6% for scapula), but even modest changes in trabecular bone mineralization are associated with much larger changes in the elastic modulus, as compressive modulus is related to the apparent density by a power of 3 (Carter & Hayes, 1977). We can infer that the tendency for decreased mineralization (i.e., TMD) in the proximal humerus likely suggests a lower compressive modulus of the trabecular bone underlying the articulating joint surfaces. Characterizing the GH joint at multiple length scales is important to improve understanding for how NBPI alters the ability to bear load in the affected bones (via changes to volumetric density, microarchitecture, and/or material properties).

Changes in joint loading are critical during the first few years of postnatal shoulder development, when the joint is mostly cartilaginous. The loads a developing joint experience will determine the type of tissues that form and their morphology (Pauwels, 1960/1980; Prendergast, Huiskes, & Søballe, 1997; Carter, Beaupré, Giori, & Helms, 1998; Loboa, Wren,

Beaupré, & Carter, 2003). Compared to a normal developing shoulder, the NBPI joint experiences increased posteriorly directed, compressive loads, as has been shown in computational musculoskeletal models (Cheng *et al*., 2015; Crouch *et al*., 2014). While full neurologic recovery occurs in 80-90% of affected children (Pearl, 2009), loads imposed on the developing joint should be closely observed. Excessive passive forces exerted on weak or paralyzed shoulders may cause mechanobiological adaptations that manifest as secondary GH deformities. In an NBPI mouse model, any paralysis endured beyond two weeks may severely impair the ability for the shoulder to recover function and develop normally (Kim *et al.*, 2009; Potter *et al.*, 2014). Bone strength in the NBPI shoulder must be sufficient to support these extrinsic loads. This holds true for the contralateral shoulder, which may be subject to overuse, as is common in other shoulder injuries like rotator cuff tears. Asymmetry during walking, as shown in a previous study with these same rats (Hennen, 2016), supports that the contralateral unaffected limb is preferentially used.

Methods to maintain or improve bone quality and strength may be necessary at these critical early years of shoulder development. Weight-bearing exercises on the affected joint, increased calcium intake (Johnston *et al*., 1992), or vitamin D supplementation (LeBoff *et al*., 1999) may delay trabecular bone losses as researchers continue to investigate the complex interactions between the neuromuscular system and bone. Extrinsic loading can support development in the weak or affected shoulder. In a study that monitored areal BMD ($g/cm^2$) in 3-5-year-old children pre- and post-treatment, the authors found that the use of neuromuscular electrical stimulation during weight-bearing exercises had a significant effect beyond weight-bearing exercises alone (Elnaggar, 2016). While volumetric measures of BMD are more

informative, the study did show that children exposed to neuromuscular stimulation had significantly improved Mallet scores.

The correlations between morphological changes and microstructural changes in the affected limb indicate that both types of measurements are similarly affected by NBPI. However, little is known about the underlying mechanisms driving these bone detriments. Altered trabecular microarchitecture may affect the joint's ability to bear loads, and likewise, altered joint loading may affect trabecular microarchitecture. Isolating contributing factors in NBPI – decreased use of the affected limb, altered muscle forces, the nerve injury itself – is crucial so that we can direct future research questions that seek to correct deformity or preserve long-term joint health. Our findings suggest that developing physical therapy or surgical treatments designed to restore proper joint loading may preserve or restore trabecular bone microarchitecture near the GH joint in addition to correcting deformity, which may improve function in the NBPI shoulder.

### 2.4.1 Limitations

Rats are an excellent model to understand the human shoulder (Soslowsky *et al*., 1996), but some differences in anatomy exist between rats and humans. Rats, for example, have two muscles, the spinodeltoid and acromiodeltoid, which are analogous to the deltoid found in humans (Wingerd, 2008). Likewise, the coracoid process of the scapula is less prominent in rats. In addition, as infants become toddlers, they transition from quadrupedal to bipedal gait, whereas rats predominantly ambulate as quadrupeds. Data analysis was not blinded and may incorporate unintended bias. Inter- or intraobserver reliability differences were not considered, but standard internal protocols were implemented to achieve consistency when reorienting and

contouring. The acromia on the scapulae from this study were removed during excision in the original study and thus were not analyzed for trabecular changes. A post-hoc power analysis revealed that an increased sample size is necessary to observe statistically significant differences ($p<0.05$) in TMD ($n=16$ per group) and Tb.Th ($n=14$ per group). Future studies employing the NBPI rat model will include contralateral limb comparisons as a way to minimize potential systemic differences between NBPI and sham limb comparisons.

To test whole bone strength, mechanical testing of the humerus and scapula should be performed. Histology of osteoblast and osteoclast activity would provide insight about how changes in bone remodeling processes contribute to the altered trabecular microarchitecture that we see. Longitudinal imaging assessments of bone and muscle would provide temporal context to the structural and mineralization changes we observed.

### 2.4.2 Summary

This thesis provides a comprehensive analysis of the trabecular bone properties near the articulating surfaces of the glenohumeral joint in an NBPI rat model. NBPI patients, who exhibit gross morphological changes to muscle and bone in the affected shoulder, demonstrate variable levels of movement and strength indicative of compromised joint loading. Trabecular bone is a crucial contributing factor in whole bone strength, which characterizes the bone's ability to bear joint loads and resist fracture. Our study reveals significantly altered trabecular bone properties in regions of the shoulder underlying the GH joint surfaces, particularly in the scapula. While fracture more commonly occurs in the clavicle as opposed to the GH bones, our study suggests that altered trabecular bone microstructure and mineralization in the humerus and scapula may be an important determinant that compromises bone strength during

the critical period of postnatal skeletal development. Post-injury care plans should prioritize bone strength for shoulder joint health in NBPI patients. Longitudinal studies are necessary to assess whether increased risk of fracture is an overlooked, unmet clinical need. Our study is a catalyst for further research to understand how nerve injury may alter trabecular bone beyond abnormal muscle loading and decreased use of the injured limb. Our study also addresses a critical need to isolate the potential direct effects of nerve injury on perinatal bone development using *in vivo* models.

# CHAPTER 3: FUTURE WORK

## 3.1 Summary

This thesis examined whether trabecular microarchitecture is altered in a rat model of NBPI. We observed trending differences in cancellous regions of the proximal humerus and several statistically significant differences in cancellous regions of the distal scapula for the NBPI affected side compared with sham controls. Both the epiphyseal and metaphyseal regions of the humerus saw a tendency for reduced trabecular thickness of approximately 12% in the NBPI group (i.e., neurectomy) relative to sham. Our data complement findings from a mouse model of NBPI, in which Tb.Th reduced by 17.6% in the neurectomy group relative to sham for 4-week-old mice (Kim *et al*., 2010). The humeral epiphysis showed a tendency for reduced tissue mineral density of 5% in our NBPI model relative to sham. Significantly less mineral accumulation in the humeral head was also noted for the NBPI mouse model (Kim *et al*., 2010), which suggests that peripheral nerve injury may disrupt normal mineral accretion in developing bone.

Interestingly, the trabecular bone in the humeral epiphysis, located immediately distal to the articulating humeral head, tended to be more severely affected than that in the metaphysis, which favors the hypothesis that abnormal postnatal skeletal growth with NPBI is modulated by altered joint loading, especially in regions closest to load-bearing surfaces. The influence of altered joint loading on bone structure has been shown indirectly via gross morphological differences in the humeral head with NBPI (e.g., flattening, subluxation from conventional articulating position in glenoid fossa) (Hoeksma *et al*., 2003.; Hogendoorn *et al*., 2010), other clinical cases of altered joint loading (e.g., bedrest (Kazakia *et al.*, 2014), spaceflight (Vico *et al.*, 2000, Lang *et al*., 2004), cerebral palsy (Marciniak, Li, & Zhou, 2015),

and in musculoskeletal simulations of the femur following developmental hip dysplasia (Shefelbine & Carter, 2004). Therefore, while the direct effects of altered joint loading following NBPI are incompletely understood, and alterations in joint loading have not yet been directly measured with NBPI, we can surmise that the changes in skeletal morphology and microarchitecture are related to altered joint loading.

To our knowledge, we present the first study characterizing the trabecular microarchitecture of the scapula in addition to the humerus in an NBPI murine model. Trabecular differences between neurectomy and sham were clearly present in each of the three ossification centers (i.e., zones) examined in this study. Increased trabecular separation of 29% was observed in the neurectomy group relative to sham in zone 1, located in the subcoracoid region that forms the superior glenoid. In zone 2, located in the inferior glenoid underlying the fossa, the neurectomy group had reduced bone volume fraction of approximately 19% relative to sham. Zone 3, also within the inferior glenoid near the glenoid rim, experienced the greatest changes, with a trend for 13% reduction in bone volume fraction, 18% reduction in trabecular number, and increased trabecular separation of 32% for neurectomy relative to sham. Zone 3 likely experiences the majority of the posteriorly directed compressive joint forces, which are generated primarily by the infraspinatus and subscapularis, as indicated by musculoskeletal computational analyses (Crouch *et al*., 2014). These two muscles have origins located on the inferior portion of the scapular body and insertions on aspects of the humeral head. Future experimental and computational studies should examine whether muscle changes are correlated with changes in trabecular bone properties to understand the relationship between altered joint loading and post-injury bone strength.

Our study reveals significantly altered trabecular bone properties in regions of the shoulder underlying the GH joint surfaces, particularly in the scapula. While fracture more commonly occurs in the clavicle as opposed to the GH bones (Ogden, 2000), following NBPI, our study suggests that altered trabecular bone mineralization and especially microstructure and mineralization in the GH bones may compromise bone strength during the critical period of postnatal skeletal development. Longitudinal studies are necessary to assess whether increased risk of fracture is an overlooked, unmet clinical need. Shoulder joint health in NBPI patients may benefit from the development of better post-injury care plans that target the maintenance of underlying trabecular bone. Our study is a catalyst for further research to understand how nerve injury may alter trabecular bone beyond abnormal muscle loading and decreased use of the injured limb. Our study also addresses a critical need to isolate the potential direct effects of nerve injury on perinatal bone development using *in vivo* models.

### 3.2 Broader Limitations

We acknowledge that limitations exist within our study design. First, rats are weight-bearing quadrupeds throughout their lifetime, while human infants outgrow crawling within the first few years of life or may even skip the crawling stage altogether and limit use of the affected limb. Gait analyses of the same rats that were used for this work (Hennen, 2016) revealed that NBPI rats exhibit different gait patterns from healthy rats and human infants (Patrick, Noah, & Yang, 2009; Righetti, Nylén, Rosander, & Ijspeert, 2015). These traits include shorter steps, increased forelimb stance width, and lower stance factor (i.e., ratio of right and left stance duration), which suggests that young NBPI rats have altered gait kinetics. The gait study performed from rats in this work (Hennen, 2016) showed significant gait

asymmetry that likely results in asymmetric joint loading (i.e., decreased ground contact with injured forelimb and increased stance duration with contralateral forelimb). Although this loading asymmetry associated with gait might not be relevant to human NBPI patients who transition to bipedal ambulation, human infants likely preferentially use their uninjured limb as they transition to using their arms for manual tasks rather than locomotion. This compensation may create future overuse injuries, as seen in patients with paraplegia (Akbar *et al.*, 2010).

This study was not powered appropriately to detect the small differences measured in trabecular TMD and Tb.Th, but a post-hoc power analysis revealed that the differences would have been statistically significant ($p<0.05$) with sample sizes of 16 per group for TMD and 14 per group for Tb.Th. These sample sizes are reasonably small and not much larger than the sample size in this study, which supports our claim that these metrics tended to decrease with NBPI compared with sham. While micro-CT analyses reveal trabecular changes between NBPI and sham shoulders, the mechanisms underlying these changes are not well understood. Histological assessments of osteoblast and osteoclast activity would provide additional insight into the underlying bone metabolism and remodeling that may be driving the trabecular bone changes with peripheral nerve injury.

Finally, nerve injury is complex. Whether nerve injury directly influences skeletal development remains an open question, one that is also confounded by cellular crosstalk between muscle and bone cells (Hamrick, McNeil, & Patterson, 2010). A recent study reported that location of nerve injury with respect to the dorsal root ganglion can have different effects on muscle spindle preservation and longitudinal muscle growth (Nikolaou *et al*., 2015), which motivates the need to examine these effects in more detail. Moreover, almost nothing is known

about the timing of nerve injury during postnatal development on the serial progression of muscle and bone deficits following injury, which may provide essential information that could lead to improved therapies in human patients.

### 3.3 Future Directions

This study informs several potential future research directions to understand mechanobiological adaptations of bone after NBPI:

- **Investigate the effect of nerve injury location with respect to the dorsal root ganglion**. Contractures are remarkably absent in patients who experience a nerve root avulsion (i.e., preganglionic) following breech delivery (Al-Qattan, 2003; Blaauw, Muhlig, Kortleve, & Tonino, 2004). In an NBPI mouse model, preganglionic injury resulted in significantly less severe elbow flexion and shoulder internal rotation contractures than postganglionic injury despite similar muscle denervation and fibrosis (Nikolaou *et al*., 2015). Observing changes in trabecular bone based on the location of nerve injury is a critical first step to understand how the neuromuscular system affects bone growth and development.
- **Investigate direct effects of nerve injury, separate from unloading effects**. Understanding the extent that nerve injury disrupts healthy bone growth and development is critical for targeting effective treatments following NBPI. A rat model is needed for comparative study. Particularly, this model should recapitulate the limited use of the affected limb via immobilization or unloading while preserving neural command to muscles that cross the shoulder.

- **Musculoskeletal modeling of the rat forelimb**. Computational tools like OpenSim (Delp *et al*., 2007) can be used to enhance our understanding of the underlying kinetics of the GH joint in rats compared to human movement simulations. Likewise, finite element analyses of shoulder joint remodeling after injury and during postnatal growth may provide new insight on how joint loads may be distributed (Shefelbine & Carter, 2004).
- **Examine bone remodeling changes of NBPI using histological techniques**. Characterizing osteoblast and osteoclast activity will add context to the changes we observed in trabecular microstructure and mineralization and lend insight to the underlying metabolic causes for these changes, which is a key first step to developing therapies that mitigate these changes.
- **Additional micro-CT analyses of other aspects of the NBPI shoulder**. To our knowledge, the growth plates and cortical bone that comprise the GH joint have not been examined but may be important in establishing the global implications of the injury to overall bone competence and weight-bearing function. In particular, analyzing the clavicle, the most common site of fracture occurring with NBPI following difficult childbirth, will be insightful for the relationship between altered trabecular bone properties and compromised bone strength following injury.
- **Mechanical testing of bone to understand structural properties and resistance to load**. Our findings suggest that bone strength is compromised, but mechanical testing mimicking *in vivo* compressive loads on the humerus and scapula is necessary to determine a direct relationship between altered trabecular bone properties and bone strength.

## REFERENCES


Abzug, J. M., Kozin, S. H., & Zlotolow, D. A. (Eds.). (2015). *The Pediatric Upper Extremity*. New York, NY: Springer New York. Retrieved from http://link.springer.com/10.1007/978-1-4614-8515-5.

Akbar, M., Balean, G., Brunner, M., Seyler, T. M., Bru.ckner, T., Munzinger, J., … Loew, M. (2010). Prevalence of rotator cuff tear in paraplegic patients compared with controls. *Journal of Bone and Joint Surgery (American)*, *92*(1), 23–31.

Al-Qattan, M. M. (2003). Obstetric Brachial Plexus Palsy Associated With Breech Delivery. *Annals of Plastic Surgery*, *51*(3), 257–64.

Anderson, M. J., Diko, S., Baehr, L. M., Baar, K., Bodine, S. C., & Christiansen, B. A. (2016). Contribution of mechanical unloading to trabecular bone loss following non-invasive knee injury in mice. *Journal of Orthopaedic Research*, *34*(10), 1680–1687. https://doi.org/10.1002/jor.23178

Bain, G. I., Itoi, E., Di Giacomo, G., & Sugaya, H. (Eds.). (2015). *Normal and Pathological Anatomy of the Shoulder*. Berlin, Heidelberg: Springer Berlin Heidelberg. Retrieved from http://link.springer.com/10.1007/978-3-662-45719-1

Bain, J. R., DeMatteo, C., Gjertsen, D., Packham, T., Galea, V., & Harper, J. A. (2012). Limb Length Differences after Obstetrical Brachial Plexus Injury: A Growing Concern. *Plastic and Reconstructive Surgery*, *130*(4), 558e–571e. https://doi.org/10.1097/PRS.0b013e318262f26b

Blaauw, G., Muhlig, R. S., Kortleve, J. W., & Tonino, A. J. (2004) Obstetric Brachial Plexus Injuries Following Breech Delivery: An Adverse Experience in The Netherlands. *Seminars in Plastic Surgery*, *18*(4), 301–7.

Berendsen, A. D., & Olsen, B. R. (2015). Bone development. *Bone*, *80*, 14–18. https://doi.org/10.1016/j.bone.2015.04.035

Bouxsein, M. L., Boyd, S. K., Christiansen, B. A., Guldberg, R. E., Jepsen, K. J., & Müller, R. (2010). Guidelines for Assessment of Bone Microstructure in Rodents Using Micro-Computed Tomography. *Journal of Bone and Mineral Research*, *25*(7), 1468-86.

Carter, D. R. & Hayes, W. C. (1977). The Compressive Behavior of Bone as a Two-Phase Porous Structure. *The Journal of Bone and Joint Surgery*, *59-A*(7), 954–62.

Carter, D. R., Beaupré, G. S., Giori, N. J., & Helms, J. A. Mechanobiology of skeletal regeneration. (1998). *Clinical Orthopaedics and Related Research*, *355*, S41–55.

Cheng, W., Cornwall, R., Crouch, D. L., Li, Z., & Saul, K. R. (2015). Contributions of Muscle Imbalance and Impaired Growth to Postural and Osseous Shoulder Deformity Following Brachial Plexus Birth Palsy: A Computational Simulation Analysis. *The Journal of Hand Surgery*, *40*(6), 1170–1176. https://doi.org/10.1016/j.jhsa.2015.02.025

Clarke, S. E., Chafetz, R. S., & Kozin, S. H. (2010). Ossification of the proximal humerus in children with residual brachial plexus birth palsy: a magnetic resonance imaging study. *Journal of Pediatric Orthopaedics*, *30*(1), 60–66.

Cole, J. H., & van der Meulen, M. C. H. (2011). Whole Bone Mechanics and Bone Quality. *Clinical Orthopaedics and Related Research®*, *469*(8), 2139–2149. https://doi.org/10.1007/s11999-011-1784-3

Cornwall, R. (2015). Glenohumeral Joint Secondary Procedures for Obstetrical Brachial Plexus Birth Palsy. In J. M. Abzug, S. H. Kozin, & D. A. Zlotolow (Eds.), *The Pediatric Upper Extremity* (pp. 633–651). Springer New York. Retrieved from http://link.springer.com.libproxy.lib.unc.edu/referenceworkentry/10.1007/978-1-4614-8515-5_29

Crouch, D. L., Hutchinson, I. D., Plate, J. F., Antoniono, J., Gong, H., Cao, G., … Saul, K. R. (2015). Biomechanical Basis of Shoulder Osseous Deformity and Contracture in a Rat Model of Brachial Plexus Birth Palsy: *The Journal of Bone and Joint Surgery-American Volume*, *97*(15), 1264–1271. https://doi.org/10.2106/JBJS.N.01247

Crouch, D. L., Plate, J. F., Li, Z., & Saul, K. R. (2014). Computational Sensitivity Analysis to Identify Muscles That Can Mechanically Contribute to Shoulder Deformity Following Brachial Plexus Birth Palsy. *The Journal of Hand Surgery*, *39*(2), 303–311. https://doi.org/10.1016/j.jhsa.2013.10.027

Delp, S. L., Anderson, F. C., Arnold, A. S., Loan, P., Habib, A., John, C. T., … Thelen, D. G. (2007). OpenSim: open-source software to create and analyze dynamic simulations of movement. *IEEE Transactions on Biomedical Engineering*, *54*(11), 1940–50. doi: 10.1109/TBME.2007.901024

Dutta, S. & Sengupta, P. (2016). Men and mice: Relating their ages. *Life Sciences*, *152*, 244–248. doi: 10.1016/j.lfs.2015.10.025

Eismann, E. A., Laor, T., & Cornwall, R. (2016). Three-Dimensional Magnetic Resonance Imaging of Glenohumeral Dysplasia in Neonatal Brachial Plexus Palsy. *The Journal of Bone & Joint Surgery*, *98*(2), 142–151. https://doi.org/10.2106/JBJS.O.00435

Elnaggar, R. K. (2016). Shoulder Function and Bone Mineralization in Children with Obstetric Brachial Plexus Injury After Neuromuscular Electrical Stimulation During Weight-Bearing Exercises. *American Journal of Physical Medicine & Rehabilitation*, *95*(4), 239–47.

Eser, P., Frotzler, A., Zehnder, Y., Wick, L., Knecht, H., Denoth, J., & Schiessl, H. (2004). Relationship between the duration of paralysis and bone structure: a pQCT study of spinal cord injured individuals. *Bone*, *34*(5), 869–880. https://doi.org/10.1016/j.bone.2004.01.001

Foad, S. L., Mehlman, C. T., & Ying, J. (2008). The Epidemiology of Neonatal Brachial Plexus Palsy in the United States. *The Journal of Bone and Joint Surgery (American)*, *90*(6), 1258–64. https://doi.org/10.2106/JBJS.G.00853

Frost, H. M. (1994) Wolff's Law and bone's structural adaptations to mechanical usage: an overview for clinicians. *The Angle Orthodontist*, *64*(3), 175–188.

Hamrick, M. W., McNeil, P. L., & Patterson, S. L. (2010). Role of muscle-derived growth factors in bone formation. *Journal of Musculoskeletal and Neuronal Interactions*, *10*(1), 64–70.

Hennen, K. K. (2016). *Effect of Severe Shoulder Deformity on Gait Characteristics in a Rat Model of Brachial Plexus Birth Palsy*. (Unpublished Masters thesis). North Carolina State University, Raleigh, NC.

Hoeksma, A. F., Ter Steeg, A. M., Dijkstra, P., Nelissen, R. G. H. H., Beelen, A., & De Jong B. A. (2003). Shoulder Contracture and Osseous Deformity in Obstetrical Brachial Plexus Injuries. *The Journal of Bone and Joint Surgery*, *85A*(2), 316–22.

Hogendoorn, S. (2010). Structural Changes in Muscle and Glenohumeral Joint Deformity in Neonatal Brachial Plexus Palsy. *The Journal of Bone and Joint Surgery (American)*, *92*(4), 935. https://doi.org/10.2106/JBJS.I.00193

Hogendoorn, S., van Overvest, K. L., Watt, I., Duijsens, A. H., & Nelissen, R. G. H. H. (2010). Structural changes in muscle and glenohumeral joint deformity in neonatal brachial plexus palsy. *The Journal of Bone and Joint Surgery-American Volume*, *92*(4), 935–942. https://doi.org/10.2106/JBJS.I.00193

Huiskes, R., Ruimerman, R., van Lenthe, G. H., & Janssen, J. D. (2000). Effects of mechanical forces on maintenance and adaptation of form in trabecular bone. *Nature*, *405*(6787), 704–6. doi: 10.1038/35015116

Iannotti, J. P. & Williams, G. R. (2007). *Disorders of the shoulder: diagnosis and management* (2nd ed.). Philadelphia, PA: Lippincott Williams & Wilkins.

Johnston, C. C., Miller, J. Z., Slemenda, C. W., Reister, T. K., Hui, S., … Peacock, M. (1992). Calcium supplementation and increases in bone mineral density in children. *New England Journal of Medicine*, *327*(2), 82–7.

Kassar-Duchossoy, L., Gayraud-Morel, B., Gomès, D., Rocancourt, D., Buckingham, M., … Tajbakhsh, S. (2004) Mrf4 determines skeletal muscle identity in Myf5: Myod double-mutant mice. *Nature*, *431*(7007), 466–71.

Kazakia, G. J., Tjong, W., Nirody, J. A., Burghardt, A. J., Carballido-Gamio, J., Patsch, J. M., … Benjamin Ma, C. (2014). The influence of disuse on bone microstructure and mechanics assessed by HR-pQCT. *Bone*, *63*, 132–140. https://doi.org/10.1016/j.bone.2014.02.014

Keaveny, T. M., Morgan, E. F., Niebur, G. L., & Yeh, O. C. (2001). Biomechanics of trabecular bone. *Annual Review of Biomedical Engineering*, *3*(1), 307–333.

Kim, H. M., Galatz, L. M., Das, R., Patel, N., & Thomopoulos, S. (2010). Musculoskeletal Deformities Secondary to Neurotomy of the Superior Trunk of the Brachial Plexus in Neonatal Mice. *Journal of Orthopaedic Research*, *28*(10), 1391–1398. https://doi.org/10.1002/jor.21128

Kim, H. M., Galatz, L. M., Patel, N., Das, R., & Thomopoulos, S. (2009). Recovery Potential After Postnatal Shoulder Paralysis: An Animal Model of Neonatal Brachial Plexus Palsy. *The Journal of Bone and Joint Surgery-American Volume*, *91*(4), 879–891. https://doi.org/10.2106/JBJS.H.00088

Kothary, S., Rosenberg, Z. S., Poncinelli, L. L., & Kwong, S. (2014). Skeletal development of the glenoid and glenoid–coracoid interface in the pediatric population: MRI features. *Skeletal Radiology*, *43*(9), 1281–1288. https://doi.org/10.1007/s00256-014-1936-0

Kozin, S. H. (2010). Brachial plexus microsurgical indications. *Journal of Pediatric Orthopaedics*, *30*, S49–S52.

Kwong, S., Kothary, S., & Poncinelli, L. L. (2014). Skeletal Development of the Proximal Humerus in the Pediatric Population: MRI Features. *American Journal of Roentgenology*, *202*(2), 418–425. https://doi.org/10.2214/AJR.13.10711

Lang, T., LeBlanc, A., Evans, H., Lu, Y., Genant, H., & Yu, A. (2004). Cortical and trabecular bone mineral loss from the spine and hip in long-duration spaceflight. *Journal of Bone and Mineral Research*, *19*(6), 1006–1012. https://doi.org/10.1359/JBMR.040307

Laplaza, F. J., Root, L., Tassanawipas, A., & Glasser, D. B. (1993). Femoral torsion and neck-shaft angles in cerebral palsy. *Journal of Pediatric Orthopaedics*, *13*(2), 192–9.

LeBoff, M. S., Kohlmeier, L., Hurwitz, S., Franklin, J., Wright, J., & Glowacki, J. (1999). Occult vitamin D deficiency in postmenopausal US women with acute hip fracture. *The Journal of the American Medical Association*, *281*(16), 1505–11.

LeGrand, E., Chappard, D., Pascaretti, C., Duquenne, M., Krebs, S., Rohmer, V., … Audran, M. (2000). Trabecular Bone Microarchitecture, Bone Mineral Density, and Vertebral Fractures in Male Osteoporosis. *Journal of Bone and Mineral Research*, *15*(1), 13–19.

Li, Z., Barnwell, J., Tan, J., Koman, L. A., & Smith, B. P. (2010). Microcomputed Tomography Characterization of Shoulder Osseous Deformity After Brachial Plexus Birth Palsy: A Rat Model Study. *The Journal of Bone and Joint Surgery (American)*, *92*(15), 2583. https://doi.org/10.2106/JBJS.I.01660

Li, Z., Ma, J., Apel, P., Carlson, C. S., Smith, T. L., & Koman, L. A. (2008). Brachial Plexus Birth Palsy–Associated Shoulder Deformity: A Rat Model Study. *The Journal of Hand Surgery*, *33*(3), 308–312. https://doi.org/10.1016/j.jhsa.2007.11.017

Liu, D., Chang-Qing, Z., Li, H., Jiang, S., Jiang, L., Dai, L. (2008). Effects of spinal cord injury and hindlimb immobilization on sublesional and supralesional bones in young growing rats. *Bone*, *43*, 119–25.

Loboa, E. G., Wren, T. A., Beaupré, G. S., & Carter, D. R. (2003) Mechanobiology of soft skeletal tissue differentiation -- a computational approach of a fiber-reinforced poroelastic model based on homogeneous and isotropic simplifications. *Biomechanics and Modeling in Mechanobiology*, *2*(2), 83–96.

Mallet J. (1972) Paralysie obstétricale du plexus brachial. Traitement des séquelles. Primaute du traitement de l'épaule—méthode d'expression des résultats. *Revue de Chirurgie Orthopédique et Réparatrice de l'Appareil Moteur*. *58S*, 166–168.

Marciniak, C., Li, X., & Zhou, P. (2015), An examination of motor unit number index in adults with cerebral palsy. *Journal of Electromyography and Kinesiology*, *25*(3), 444–50.

McDaid, P. J., Kozin, S. H., Thoder, J. J., & Porter, S. T. (2002). Upper extremity limb-length discrepancy in brachial plexus palsy. *Journal of Pediatric Orthopaedics*, *22*(3), 364–366.

Moore, K. L. & Dalley, A. F. (1999). *Clinical Oriented Anatomy* (4th ed.). New York, NY: Lippincott Williams & Wilkins.

Mullender, M. G., Huiskes, R., & Weinans, H. (1994). A physiological approach to the simulation of bone remodeling as a self-organizational control process. *Journal of Biomechanics*, *27*(11): 1389–94.

Nikolaou, S., Hu, L., & Cornwall, R. (2015). Afferent Innervation, Muscle Spindles, and Contractures Following Neonatal Brachial Plexus Injury in a Mouse Model. *The Journal of Hand Surgery*, *40*(10), 2007–2016. https://doi.org/10.1016/j.jhsa.2015.07.008

Nikolaou, S., Peterson, E., Kim, A., Wylie, C., & Cornwall, R. (2011). Impaired Growth of Denervated Muscle Contributes to Contracture Formation Following Neonatal Brachial Plexus Injury: *The Journal of Bone and Joint Surgery-American Volume*, *93*(5), 461–470. https://doi.org/10.2106/JBJS.J.00943

Norlin, R., Hoe-Hansen, C., Oquist, G., & Hildebrand C. (1994). Shoulder region of the rat: anatomy and fiber composition of some suprascapular nerve branches. *The Anatomical Record*, *239*(3), 332–42.

Nowlan, N. C., Bourdon, C., Dumas, G., Tajbakhsh, S., Prendergast, P. J., & Murphy, P. (2010). Developing bones are differentially affected by compromised skeletal muscle formation. *Bone*, *46*(5), 1275–1285. https://doi.org/10.1016/j.bone.2009.11.026

Ogden, J. A. & Phillips, S. B. (1983). Radiology of Postnatal Skeletal Development VII. The Scapula. *Skeletal Radiology*, *9*, 157–69.

Ogden, J. A. (2000). *Skeletal Injury in the Chlid* (3rd ed.). New York, NY: Springer.

Parfitt, A. M., Mathews, C. H., Villanueva, A. R., Kleerekoper, M., Frame, B., & Rao, D. S. (1983). Relationships between surface, volume, and thickness of iliac trabecular bone in aging and in osteoporosis. Implications for the microanatomic and cellular mechanisms of bone loss. *The Journal of Clinical Investigation*, *72*(4), 1396–1409. doi: 10.1172/JCI111096.

Patrick, S. K., Noah, J. A., & Yang, J. F. (2009). Interlimb Coordination in Human Crawling Reveals Similarities in Development and Neural Control with Quadrupeds. *Journal of Neurophysiology*, *101*(2), 603–13.

Pauwels, F. (1980). *A new theory concerning the influence of mechanical stimuli on the differentiation of the supporting tissues*. (R. Furlong & P. Maquet, Trans.). Berlin, Heidelberg: Springer Berlin Heidelberg. (Original work published 1960)

Pearl, M. L., Edgerton, B. W., Kon, D. S., Darakijan, A. B., Kosco, A. E., … Burchette, R. J. (2003). Comparison of Arthroscopic Findings with Magnetic Resonance Imaging and Arthrography in Children with Glenohumeral Deformities Secondary to Brachial Plexus Birth Palsy. *The Journal of Bone and Joint Surgery*, *85*(5), 890–98.

Pearl, M. L. (2009). Shoulder problems in children with brachial plexus birth palsy: evaluation and management. *Journal of the American Academy of Orthopaedic Surgeons*, *17*(4), 242–254.

Poliachik, S. L., Bain, S. D., Threet, D., Huber, P., Gross, T. S. (2010). Transient muscle paralysis disrupts bone homeostasis by rapid degradation of bone morphology. *Bone, 46*, 18–23.

Potter, R., Havlioglu, N., & Thomopoulos, S. (2014). The developing shoulder has a limited capacity to recover after a short duration of neonatal paralysis. *Journal of Biomechanics*, *47*(10), 2314–2320. https://doi.org/10.1016/j.jbiomech.2014.04.036

Prendergast, P. J., Huiskes, R. Prendergast, & Søballe, K. (1997) ESB Research Award 1996. Biophysical stimuli on cells during tissue differentiation at implant interfaces. *Journal of Biomechanics*, *30*(6), 539–48.

Quinn, R. (2005). Comparing rat's to human's age: how old is my rat in people years? *Nutrition*, *21*, 775–777.

Reading, B. D., Laor, T., Salisbury, S. R., Lippert, W. C., & Cornwall, R. (2012). Quantification of Humeral Head Deformity Following Neonatal Brachial Plexus Palsy. *The Journal of Bone and Joint Surgery (American)*, *94*(18), e136(1-8). https://doi.org/10.2106/JBJS.K.00540.

Righetti, L., Nylén, A., Rosander, K., & Ijspeert, A. J. (2015). Kinematic and Gait Similarities between Crawling Human Infants and Other Quadruped Mammals. *Frontiers in Neurology*, *6*(17). doi: 10.3389/fneur.2015.00017

Rockwood, C. A. & Matsen, F. A. *The shoulder* (4th ed.). Philadelphia, PA: Saunders.

Roux, W. (1895) *Gesammelte Abhandlungen über Entwickelungsmechanik der Organismen*. Leipzig: Engelmann.

Shefelbine, S. J. & Carter, D. R. (2004). Mechanobiological predictions of growth front morphology in developmental hip dysplasia. *Journal of Orthopaedic Research*, *22*(2), 346–52.

Sibinski, M., Woźniakowski, B., Drobniewski, M., & Synder, M. (2010). Secondary glenohumeral joint dysplasia in children with persistent obstetric brachial plexus palsy. *International Orthopaedics*, *34*(6), 863–867. https://doi.org/10.1007/s00264-010-0965-0

Soldado, F., & Kozin, S. H. (2005). The relationship between the coracoid and glenoid after brachial plexus birth palsy. *Journal of Pediatric Orthopaedics*, *25*(5), 666–670.

Soslowsky, L. J. Carpenter, J. E., DeBano, C. M., Banerji, I., & Moalli, M. R. Development and use of an animal model for investigations on rotator cuff disease. *Journal of Shoulder and Elbow Surgery, 5*, 383–92.

Stein, E. M., Kepley, A., Walker, M., Nickolas, T. L., Nishiyama, K., Zhou, B., … Shane, E. (2014). Skeletal structure in postmenopausal women with osteopenia and fractures is characterized by abnormal trabecular plates and cortical thinning. *Journal of Bone and Mineral Research*, *29*(5), 1101–9.

Tajbakhsh, S., Rocancourt, D., Cossu, G., & Buckingham M. (1997). Redefining the genetic hierarchies controlling skeletal myogenesis: Pax-3 and Myf-5 act upstream of MyoD. *Cell*, *89*(1), 127–38.

Turner, C. H. (1998). Three rules for bone adaptation to mechanical stimuli. *Bone*, *23*(5), 399–407.

van der Meulen, M. C. H., Jepsen, K. J., & Mikić, B. (2001). Understanding Bone Strength: Size Isn't Everything. *Bone*, *29*(2), 101–4.

van der Slujis, J. A., van Ouwerkerk, W. J., de Gast, A., Wuisman, P. I., Nollet F., & Manoliu, R.A. (2001). Deformities of the shoulder in infants younger than 12 months with an obstetric lesion of the brachial plexus. *Journal of Bone and Joint Surgery (British)*, *83*(4), 551–5.

van Gelein Vitringa, V., van Kooten, E., Mullender, M., van Doorn-Loogman, M., & van der Sluijs, J. (2009). An MRI study on the relations between muscle atrophy, shoulder function and glenohumeral deformity in shoulders of children with obstetric brachial plexus injury. *Journal of Brachial Plexus and Peripheral Nerve Injury*, *4*(1), e21–e28. https://doi.org/10.1186/1749-7221-4-5

Vico, L., Collet, P., Guignandon, A., Lafage-Proust, M.-H., Thomas, T., Rehailia, M., & Alexandre, C. (2000). Effects of long-term microgravity exposure on cancellous and cortical weight-bearing bones of cosmonauts. *The Lancet*, *355*(9215), 1607–1611. https://doi.org/10.1016/S0140-6736(00)02217-0

Waters, P. M., Monica, J. T., Earp, B. E., Zurakowski, D., & Bae, D. S. (2009). Correlation of Radiographic Muscle Cross-Sectional Area with Glenohumeral Deformity in Children with Brachial Plexus Birth Palsy: *The Journal of Bone and Joint Surgery-American Volume*, *91*(10), 2367–2375. https://doi.org/10.2106/JBJS.H.00417

Waters, P. M., Smith, G. R., & Jaramillo, D. (1998). Glenohumeral deformity secondary to brachial plexus birth palsy. *The Journal of Bone and Joint Surgery. American Volume*, *80*(5), 668–677.

Wingerd, B. D. (2008) *Rat anatomy and dissection guide*. Minneapolis, MN: Bluedoor.

Weekley, H., Nikolaou, S., Hu, L., Eismann, E., Wylie, C., & Cornwall, R. (2012). The effects of denervation, reinnervation, and muscle imbalance on functional muscle length and elbow flexion contracture following neonatal brachial plexus injury. *Journal of Orthopaedic Research*, *30*(8), 1335–1342. https://doi.org/10.1002/jor.22061

Wolff, J. (1986). *The Law of Bone Remodelling*. (R. Furlong & P. Maquet, Trans.). Berlin, Heidelberg: Springer Berlin Heidelberg. (Original work published 1892)

Yang, L., Tsang, K. Y., Tang, H. C., Chan, D., & Cheah, K. S. Hypertrophic chondrocytes can become osteoblasts and osteocytes in endochodral bone formation. *Proceedings of the National Academy of Sciences of the United States of America*, *111*(33), 12097-102. doi: 10.1073/pnas.1302703111

Yaraskavitch, M., Leonard, T., & Herzog, W. (2008). Botox produces functional weakness in non-injected muscles adjacent to the target muscle. *Journal of Biomechanics*, *41*(4), 897–902. https://doi.org/10.1016/j.jbiomech.2007.11.016

Zember, J. S., Rosenberg, Z. S., Kwong, S., Kothary, S. P., & Bedoya, M. A. (2015). Normal Skeletal Maturation and Imaging Pitfalls in the Pediatric Shoulder. *RadioGraphics*, *35*(4), 1108–1122. https://doi.org/10.1148/rg.2015140254

Zhou, B. O., Yue, R., Murphy, M. M., Peyer, J. G., & Morrison, S. J. (2014). Leptin-receptor-expressing mesenchymal stromal cells represent the main source of bone formed by adult bone marrow. *Cell Stem Cell*, *15*(2), 154-68. doi: 10.1016/j.stem.2014.06.008